Legends for Figures

Fig 1.
Unfractionated PBMCs can serve as a source of functional myeloid DCs *in vitro*.
Purified monocytes or PBMCs were cultured at 5 x 10^5 and 2.5 x 10^6 cells/ml, respectively, in media containing GM-CSF and IL-4 for 5 days followed by maturation by incubation with poly I:C and IL-1β for an additional 2 days. (a) Representative phenotypic profile of the matured cells as determined by flow cytometry is shown. Mo-DC from purified monocytes, and PB-DC from bulk PBMCs. (b)The T cell stimulating activity of the matured DCs was analyzed by co-culture with CFSE-labeled purified allogeneic $CD4^+$ T cells at a DC to T cell ratio of 1:50 in RPMI medium containing 20 U/ml IL-2 in U-bottom 96-well plates for 4 days. Proliferation of the CFSE-labeled $CD4^+$ T cells was assayed by flow cytometry. Data shown are representative of three independent experiments utilizing blood from 3 different donors.

Fig 2.
Exposure of PBMCs to iHIV-1 impairs DC generation.
Highly enriched populations of monocytes and bulk PBMCs were cultured as described in Fig.1 in the presence or absence of iHIV-1.
(a) Cultures of DCs generated from monocytes or PBMCs either in the presence or absence of iHIV-$1_{JR\text{-}CSF}$ (50 ng/ml p24 level) were visualized on day 5 using an inverted microscope (200x).
(b) The impairment of DC generation from PBMCs in the presence of various concentrations of iHIV-$1_{JR\text{-}CSF}$ added at the initiation of cultures. On day 5, cells were analyzed by flow cytometry. Note that normal DCs have a high FSC and high SSC profile. The profiles of CD11c and CD86 expression by un-gated PBMCs and statistical analysis of $\%CD11c^+$ cells was shown.
(c) Time course of HIV-1-mediated impairment of DC generation from PBMCs. PBMCs cultured in the presence or absence of iHIV-$1_{JR\text{-}CSF}$ (at 50 ng/ml p24 level) as in Fig.1, and the FSC and high SSC profile and %CD11c+ cells in un-gated PBMCs were examined on days 3, 4 and 5.
(d) PBMCs cultured in the presence or absence of iHIV-$1_{JR\text{-}CSF}$ (at 50 ng/ml p24 level) were examined for $CD14^+$ monocyte apoptosis on day 1 by CD14 and Annexin-V staining. Gates were set based on background profile of cells incubated with Annexin-V on day 0.
Data shown are representatives of three independent experiments utilizing blood from 3 different donors.

Fig 3.
Both CCR5- and CXCR4-tropic iHIV-1 isolates impair DC generation from PBMCs and modify CD86 expression.
Aliquots of highly enriched preparation of monocytes and unfractionated PBMCs were cultured as in Fig.1 in the presence or absence of AT-2 inactivated CCR5-tropic HIV-$1_{JR\text{-}CSF}$ or CXCR4-tropic HIV-1_{IIIB} each at 50 ng/ml p24 level for 5 days.
(a) The total number of viable $CD11c^+$DCs were determined as described in the "Material and Methods" section and data expressed as percent viable cells.
(b) The levels of CD86 expression on DCs was determined by flow cytometry and are shown as the mean fluorescence intensity (MFI).
Representative data from 3 different donors are shown.

Fig 4.
DCs generated from iHIV-1-exposed PBMC cultures are less potent in IFN-γ production than those from control cultures.
Unfractionated PBMCs (PB-DC) or monocyte derived DC's (Mo-DC's) were cultured in the presence or absence of iHIV-$1_{JR\text{-}CSF}$ (50 ng/ml of p24) for 5 days as described under Fig.1. The resulting DCs were then co-cultured with allogeneic bulk T cells at a DC:T ratio of 1:50 in RPMI medium containing 20 U/ml IL-2 in U-bottom 96 well-plates for 4 days. The supernatants were assayed for IFN-γ, IL-10 and IL-4 production by ELISA. All results are expressed as the mean ± standard deviation from three independent experiments. Representative data from 3 different donors are shown.

Fig 5.
Type-I IFNs impair DC generation in both unfractionated PBMCs and monocytes.
Highly enriched preparation of monocytes and unfractionated PBMCs were pretreated with either (a) medium alone

or (b) 10 ug/ml anti IFN-receptor 2 (IFNR2) antibody for 30 min at 37°C, and then, without washing, cultured as in the Fig.1 in the presence or absence of type-1 IFNs (5 ng/ml IFN-α) or IFN-β, 5 ng/ml each), 20 ug/ml poly I:C or iHIV-1_{JR-CSF} (at 50 ng/ml p24) for 5 days, and the total number of viable $CD11c^+$ DC and the relative level (MFI) of CD86 expression determined. As IFN-α, 5 ng/ml IFN-β showed similar results (data not shown).
Representative data from 3 different donors are shown.

Fig 6.
HIV-1 induces IFN-α but not IFN-β from $CD123^+$ plasmacytoid DCs in unfractionated PBMCs.
(a) Unfractionated PBMCs and highly enriched preparation of monocytes were cultured as in the Fig.1 either in the presence or absence of iHIV-1_{JR-CSF} (50 ng/ml of p24) or poly I:C for 3 days, and the level of IFN-α production in the culture supernatants was determined by ELISA.
(b) Unfractionated PBMCs or PBMCs depleted of $CD123^+$ cells were cultured either in the presence or absence of iHIV-1_{JR-CSF} (50 ng/ml of p24) for 5 days, and the total number of viable $CD11c^+$DC determined.
All results are expressed as the mean ± standard deviation from three independent experiments. Representative data from 3 different donors are shown.

Fig 7.
iHIV-1 impairs DC generation from PBMCs in a CD4 dependent fashion.
Aliquots of unfractionated PBMCs were pretreated with either 20 ug/ml anti-CD4 mAb or control IgG for 30 min at 37°C, and subsequently, without washing, cultured as in the Fig.1 either in the absence or presence of inactivated HIV-1_{JR-CSF} (at 50 ng/ml p24) for 5 days, and aliquots evaluated for the total number of viable $CD11c^+$DCs (a), elative levels of CD86 expression (b). The levels of IFN-α production in the culture supernatants collected on day 3 were determined by ELISA.
All results are expressed as the mean ± standard deviation from three independent experiments. Representative data from 3 different donors are shown.

Fig 8. iHIV-1-mediated impairment of DC generation is reversed by TNF but not by antibodies against TRAIL, Fas ligand, TNF-α, TNF-β or TNF receptor.
(a) Aliquots of unfractionated PBMCs were either untreated or pretreated with 5 ug/ml of anti-TRAIL mAb, anti-FasL, anti-TNF-α, anti-TNF-β or anti-TNF receptor-I at 37°C for 30 min, and subsequently, without washing, cultured as in the Fig.1 either in the absence or presence of iHIV-1_{JR-CSF} (at 50 ng/ml p24) for 5 days. The total numbers of viable $CD11c^+$ DC were then determined.
(b) Unfractionated PBMCs were cultured as in Fig.1 either in the presence or absence of 5 ng/ml IFN-α, 20 ug/ml poly I:C or iHIV-1_{JR-CSF} (50 ng/ml of p24) for 5 days either with 20 ng/ml TNF (α or β), and then the total number of viable $CD11c^+$ DC determined.
(c) IFN-α production in the culture supernatants (except from the IFN-α added cultures) from Fig.8(b) was determined on day 3 by ELISA
All results are expressed as the mean ± standard deviation from three independent experiments.

References

[1] Schuler G, Schuler-Thurner B, Steinman RM: The use of dendritic cells in cancer immunotherapy. Curr Opin Immunol 2003;15:138-47.

[2] Banchereau J, Palucka AK: Dendritic cells as therapeutic vaccines against cancer. Nat Rev Immunol 2005;5:296-306.

[3] Figdor CG, de Vries IJ, Lesterhuis WJ, Melief CJ: Dendritic cell immunotherapy: mapping the way. Nat Med 2004;10:475-480.

[4] Lu W, Wu X, Lu Y, Guo W, Andrieu JM: Therapeutic dendritic-cell vaccine for simian AIDS. Nat 2003;9:27-32.

[5] Yoshida A, Tanaka R, Murakami T, Takahashi Y, Koyanagi Y, Nakamura M, Ito M, Yamamoto N, Tanaka Y: Induction of protective immune responses against R5 human immunodeficiency virus type 1 (HIV-1) infection in hu-PBL-SCID mice by intrasplenic immunization with HIV-1-pulsed dendritic cells: possible involvement of a novel factor of human CD4(+) T-cell origin. J Virol 2003;77:8719-8728.

[6] Lapenta C, Santini SM, Logozzi M, Spada M, Andreotti M, Di Pucchio T, Parlato S, Belardelli F: Potent immune response against HIV-1 and protection from virus challenge in hu-PBL-SCID mice immunized with inactivated virus-pulsed dendritic cells generated in the presence of IFN-α. J Exp Med 2003;198:361-367

[7] Ide F, Nakamura T, Tomizawa M, Kawana-Tachikawa A, Odawara T, Hosoya N, Iwamoto A: Peptide-loaded dendritic-cell vaccination followed by treatment interruption for chronic HIV-1 infection: a phase 1 trial. J Med Virol 2006;78:711-718.

[8] Donaghy H, Pozniak A, Gazzard B, Qazi N, Gilmour J, Gotch F, Patterson S: Loss of blood CD11c(+) myeloid and CD11c(-) plasmacytoid dendritic cells in patients with HIV-1 infection correlates with HIV-1 RNA virus load. Blood 2001;98:2574-2576.

[9] Pacanowski J, Kahi S, Baillet M, Lebon P, Deveau C, Goujard C, Meyer L, Oksenhendler E, Sinet M, Hosmalin A: Reduced blood CD123+ (lymphoid) and CD11c+ (myeloid) dendritic cell numbers in primary HIV-1 infection. Blood 2001;98:3016-3021.

[10] Fernandez S, Stone SF, Price P, French MA: The number and function of circulating dendritic cells may limit effector memory CD4+ T-cell responses in HIV patients responding to antiretroviral therapy. Clin Immunol 2008;128:228-237.

[11] Fontaine J, Coutlee F, Tremblay C, Routy JP, Poudrier J, Roger M: HIV infection affects blood myeloid dendritic cells after successful therapy and despite nonprogressing clinical disease. J Infect Dis 2009;199:1007-1018.

[12] Chehimi J, Campbell DE, Azzoni L, Bacheller D, Papasavvas E, Jerandi G, Mounzer K, Kostman J, Trinchieri G, Montaner LJ: Persistent decreases in blood plasmacytoid dendritic cell number and function despite effective highly active antiretroviral therapy and increased blood myeloid dendritic cells in HIV-infected individuals. J Immunol 2002;168:4796-4801.

[13] Finke JS, Shodell M, Shah K, Siegal FP, Steinman RM: Dendritic cell numbers in the blood of HIV-1 infected patients before and after changes in antiretroviral therapy. J Clin Immunol 2004;24:647-652.

[14] Ahlers JD, Belyakov IM: Strategies for recruiting and targeting dendritic cells for optimizing HIV vaccines. Trends Mol Med 2009;15:263-274.

[15] Dai B, Yang L, Yang H, Hu B, Baltimore D, Wang P: HIV-1 Gag-specific immunity induced by a lentivector-based vaccine directed to dendritic cells. Proc Natl Acad Sci U S A 2009;106:20382-20387.

[16] Kloverpris H, Karlsson I, Bonde J, Thorn M, Vinner L, Pedersen AE, Hentze JL, Andresen BS, Svane IM, Gerstoft J, Kronborg G, Fomsgaard A: Induction of novel CD8+ T-cell responses during chronic untreated HIV-1 infection by immunization with subdominant cytotoxic T-lymphocyte epitopes. AIDS 2009;23:1329-1340.

[17] Timmerman JM, Czerwinski DK, Davis TA, Hsu FJ, Benike C, Hao ZM, Taidi B, Rajapaksa R, Caspar CB, Okada CY, van Beckhoven A, Liles TM, Engleman EG, Levy R: Idiotype-pulsed dendritic cell vaccination for B-cell lymphoma: clinical and immune responses in 35 patients. Blood 2002;99:1517-1526.

[18] Jonuleit H, Giesecke-Tuettenberg A, Tuting T, Thurner-Schuler B, Stuge TB, Paragnik L, Kandemir A, Lee PP, Schuler G, Knop J, Enk AH: A comparison of two types of dendritic cell as adjuvants for the induction of melanoma-specific T-cell responses in humans following intranodal injection. Int J Cancer 2001;93:243-251.

[19] Berger TG, Strasser E, Smith R, Carste C, Schuler-Thurner B, Kaempgen E, Schuler G: Efficient elutriation of monocytes within a closed system (Elutra) for clinical-scale generation of dendritic cells. J Immunol Methods 2005;298:61-72.

[20] Babatz J, Rollig C, Oelschlagel U, Zhao S, Ehninger G, Schmitz M, Bornhauser M: Large-scale immunomagnetic selection of CD14+ monocytes to generate dendritic cells for cancer immunotherapy: a phase I study. J Hematother Stem Cell Res 2003;12:515-523.
[21] Sallusto F, Lanzavecchia A: Efficient presentation of soluble antigen by cultured human dendritic cells is maintained by granulocyte/macrophage colony-stimulating factor plus interleukin 4 and downregulated by tumor necrosis factor α. J Exp Med 1994;179:1109-1118.
[22] Tawab A, Fan Y, Read EJ, Kurlander RJ: Effect of *ex vivo* culture duration on phenotype and cytokine production by mature dendritic cells derived from peripheral blood monocytes. Transfusion 2009;49:536-547.
[23] Koski GK, Lyakh LA, Rice NR: Rapid lipopolysaccharide-induced differentiation of CD14(+) monocytes into CD83(+) dendritic cells is modulated under serum-free conditions by exogenously added IFN-γ and endogenously produced IL-10. Eur J Immunol 2001;31:3773-3781.
[24] Dauer M, Obermaier B, Herten J, Haerle C, Pohl K, Rothenfusser S, Schnurr M, Endres S, Eigler A: Mature dendritic cells derived from human monocytes within 48 hours: a novel strategy for dendritic cell differentiation from blood precursors. J Immunol 2003;170:4069-4076.
[25] Zhang LF, Okuma K, Tanaka R, Kodama A, Kondo K, Ansari AA, Tanaka Y: Generation of mature dendritic cells with unique phenotype and function by *in vitro* short-term culture of human monocytes in the presence of interleukin-4 and interferon-β. Exp Biol Med (Maywood) 2008;233:721-731.
[26] Dhodapkar MV, Steinman RM, Sapp M, Desai H, Fossella C, Krasovsky J, Donahoe SM, Dunbar PR, Cerundolo V, Nixon DF, Bhardwaj N: Rapid generation of broad T-cell immunity in humans after a single injection of mature dendritic cells. J Clin Invest 1999;104:173-180.
[27] Lehner M, Felzmann T, Clodi K, Holter W: Type I interferons in combination with bacterial stimuli induce apoptosis of monocyte-derived dendritic cells. Blood 2001;98:736-742.
[28] McRae BL, Nagai T, Semnani RT, van Seventer JM, van Seventer GA: Interferon-α and -β inhibit the *in vitro* differentiation of immunocompetent human dendritic cells from CD14(+) precursors. Blood 2000;96:210-217.
[29] Goxe B, Latour N, Chokri M, Abastado JP, Salcedo M: Simplified method to generate large quantities of dendritic cells suitable for clinical applications. Immunol Invest 2000;29:319-336.
[30] Lund PK, Westvik AB, Joo GB, Ovstebo R, Haug KB, Kierulf P: Flow cytometric evaluation of apoptosis, necrosis and recovery when culturing monocytes. J Immunol Methods 2001;252:45-55.
[31] Lund PK, Namork E, Brorson SH, Westvik AB, Joo GB, Ovstebo R, Kierulf P: The fate of monocytes during 24 h of culture as revealed by flow cytometry and electron microscopy. J Immunol Methods 2002;270:63-76.
[32] Mangan DF, Wahl SM: Differential regulation of human monocyte programmed cell death (apoptosis) by chemotactic factors and pro-inflammatory cytokines. J Immunol 1991;147:3408-3412.
[33] Fahy RJ, Doseff AI, Wewers MD: Spontaneous human monocyte apoptosis utilizes a caspase-3-dependent pathway that is blocked by endotoxin and is independent of caspase-1. J Immunol 1999;163:1755-1762.
[34] Bohnenkamp HR, Burchell JM, Taylor-Papadimitriou J, Noll T: Apoptosis of monocytes and the influence on yield of monocyte-derived dendritic cells. J Immunol Methods 2004;294:67-80.
[35] Yen JH, Ganea D: Interferon β induces mature dendritic cell apoptosis through caspase-11/caspase-3 activation. Blood 2009;114:1344-1354.
[36] Luft T, Pang KC, Thomas E, Hertzog P, Hart DN, Trapani J, Cebon J: Type I IFNs enhance the terminal differentiation of dendritic cells. J Immunol 1998;161:1947-1953.
[37] Paquette RL, Hsu NC, Kiertscher SM, Park AN, Tran L, Roth MD, Glaspy JA: Interferon-α and granulocyte-macrophage colony-stimulating factor differentiate peripheral blood monocytes into potent antigen-presenting cells. J Leukoc Biol 1998;64:358-367.
[38] Santini SM, Lapenta C, Logozzi M, Parlato S, Spada M, Di Pucchio T, Belardelli F: Type I interferon as a powerful adjuvant for monocyte-derived dendritic cell development and activity *in vitro* and in Hu-PBL-SCID mice. J Exp Med 2000;191:1777-1788.
[39] Dauer M, Pohl K, Obermaier B, Meskendahl T, Robe J, Schnurr M, Endres S, Eigler A: Interferon-α disables dendritic cell precursors: dendritic cells derived from interferon-α-treated monocytes are defective in maturation and T-cell stimulation. Immunology 2003;110:38-47.
[40] Gauzzi MC, Canini I, Eid P, Belardelli F, Gessani S: Loss of type I IFN receptors and impaired IFN responsiveness during terminal maturation of monocyte-derived human dendritic cells. J Immunol 2002;169:3038-3045.
[41] Ferbas JJ, Toso JF, Logar AJ, Navratil JS, Rinaldo CR, Jr.: CD4+ blood dendritic cells are potent producers of IFN-α in response to *in vitro* HIV-1 infection. J Immunol 1994;152:4649-4662.
[42] Francis ML, Meltzer MS: Induction of IFN-α by HIV-1 in monocyte-enriched PBMC requires gp120-CD4

interaction but not virus replication. J Immunol 1993;151:2208-2216.
[43] Beignon AS, McKenna K, Skoberne M, Manches O, DaSilva I, Kavanagh DG, Larsson M, Gorelick RJ, Lifson JD, Bhardwaj N: Endocytosis of HIV-1 activates plasmacytoid dendritic cells via Toll-like receptor-viral RNA interactions. J Clin Invest 2005;115:3265-3275.
[44] Haupt S, Donhauser N, Chaipan C, Schuster P, Puffer B, Daniels RS, Greenough TC, Kirchhoff F, Schmidt B: CD4 binding affinity determines human immunodeficiency virus type 1-induced α interferon production in plasmacytoid dendritic cells. J Virol 2008;82:8900-8905.
[45] Martinelli E, Cicala C, Van Ryk D, Goode DJ, Macleod K, Arthos J, Fauci AS: HIV-1 gp120 inhibits TLR9-mediated activation and IFN-α secretion in plasmacytoid dendritic cells. Proc Natl Acad Sci U S A 2007;104:3396-3401.
[46] Fonteneau JF, Larsson M, Beignon AS, McKenna K, Dasilva I, Amara A, Liu YJ, Lifson JD, Littman DR, Bhardwaj N: Human immunodeficiency virus type 1 activates plasmacytoid dendritic cells and concomitantly induces the bystander maturation of myeloid dendritic cells. J Virol 2004;78:5223-5232.
[47] Morse MA, Zhou LJ, Tedder TF, Lyerly HK, Smith C: Generation of dendritic cells *in vitro* from peripheral blood mononuclear cells with granulocyte-macrophage-colony-stimulating factor, interleukin-4, and tumor necrosis factor-α for use in cancer immunotherapy. Ann Surg 1997;226:6-16.
[48] Semnani RT, Venugopal PG, Mahapatra L, Skinner JA, Meylan F, Chien D, Dorward DW, Chaussabel D, Siegel RM, Nutman TB: Induction of TRAIL- and TNF-α-dependent apoptosis in human monocyte-derived dendritic cells by microfilariae of Brugia malayi. J Immunol 2008;181:7081-7089.
[49] Baldwin HM, Ito-Ihara T, Isaacs JD, Hilkens CM: TNFα blockade impairs dendritic cell survival and function in rheumatoid arthritis. Ann Rheum Dis 2009 in press.

Fig.1

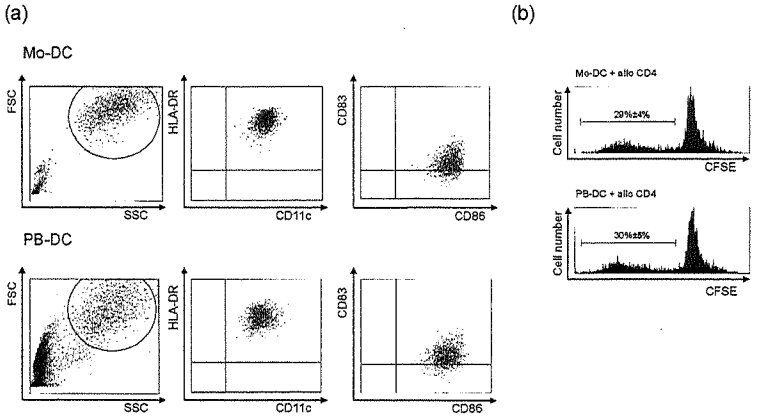

Fig.2

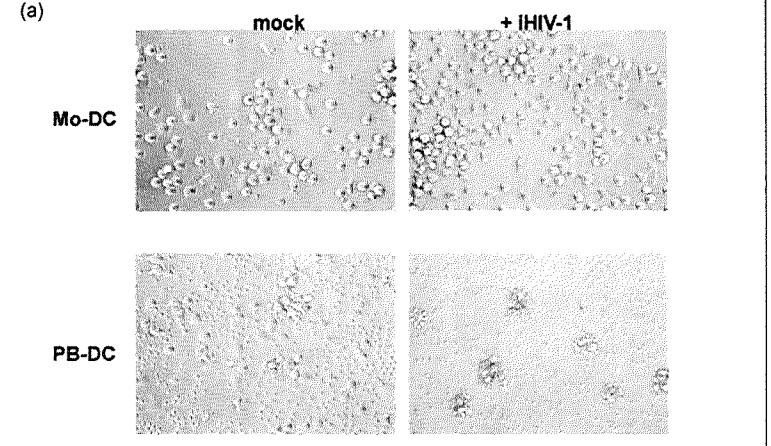

Fig.2 continued

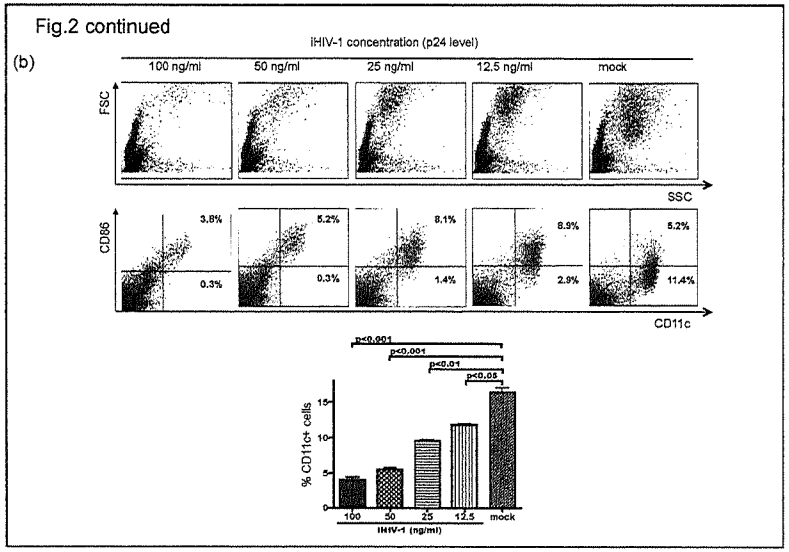

Fig.2 continued

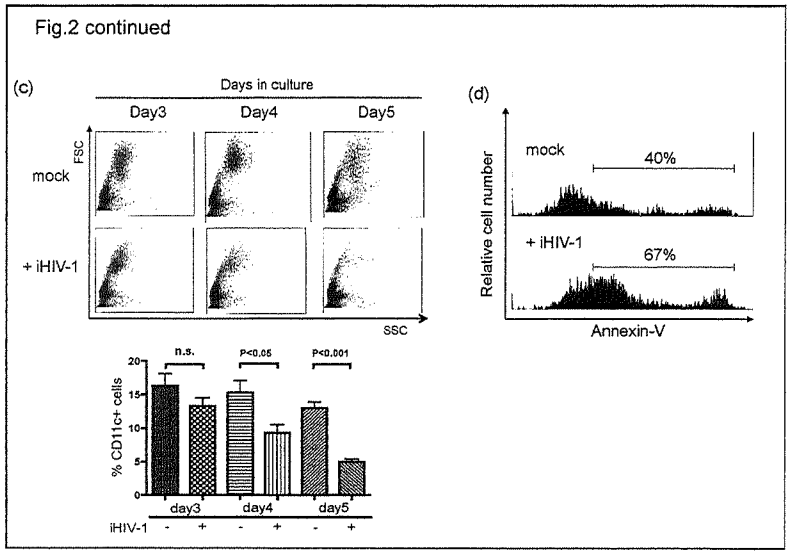

Fig.3

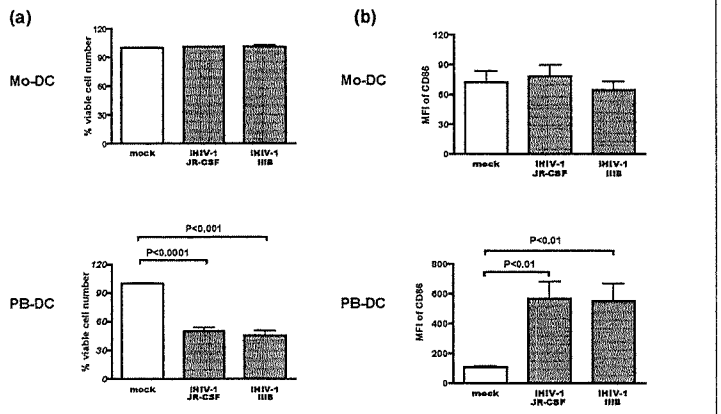

Fig.4

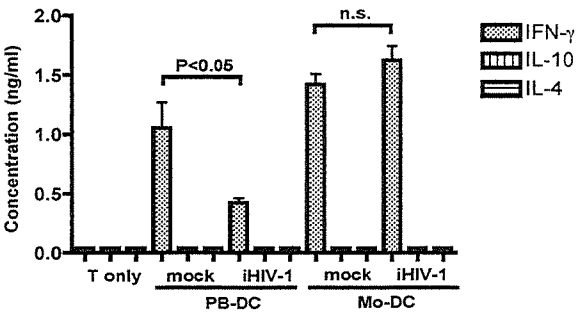

Fig.5

(a)

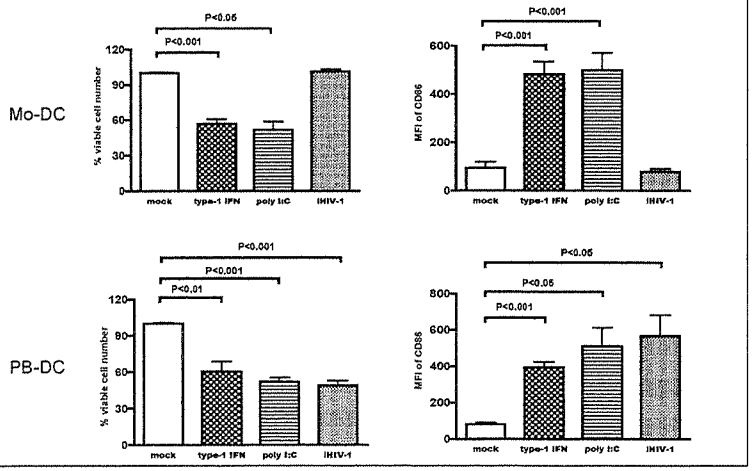

Fig.5 continued

(b)

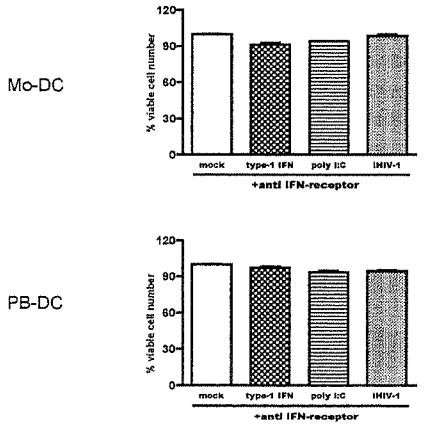

Fig.6

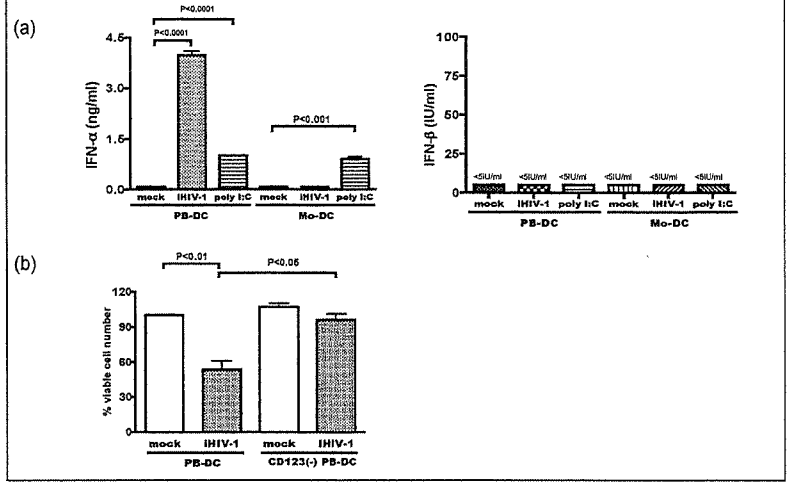

Fig.7

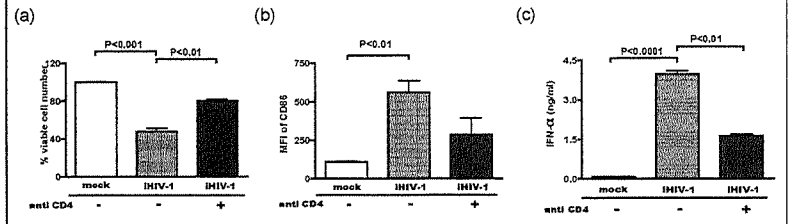

Fig.8

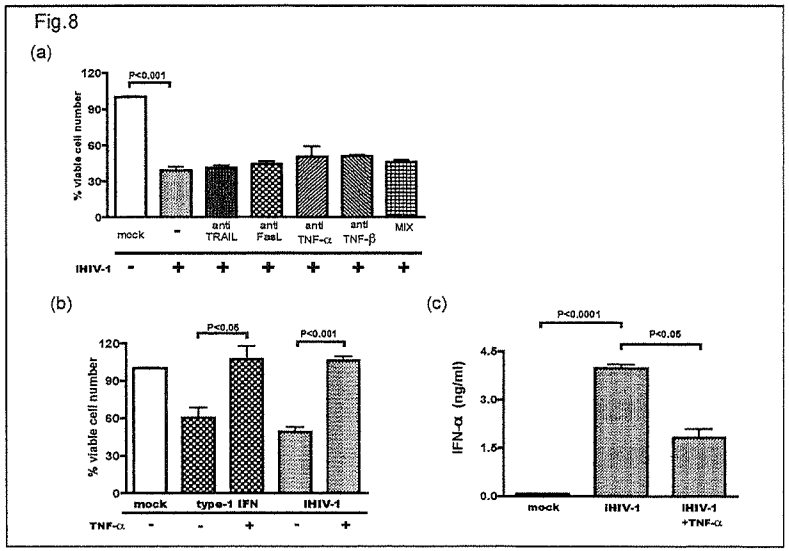

Vaccine xxx (2009) xxx–xxx

Contents lists available at ScienceDirect

Vaccine

journal homepage: www.elsevier.com/locate/vaccine

Dynamics of memory and naïve CD8$^+$ T lymphocytes in humanized NOD/SCID/IL-2Rγ^{null} mice infected with CCR5-tropic HIV-1

Kei Sato[a,1], Chuanyi Nie[a,1], Naoko Misawa[a,1], Yuetsu Tanaka[b], Mamoru Ito[c], Yoshio Koyanagi[a,*]

[a] Laboratory of Viral Pathogenesis, Institute for Virus Research, Kyoto University, Kyoto 606-8507, Japan
[b] Department of Immunology, Graduate School of Medicine, University of the Ryukyus, Nishihara, Okinawa 903-0125, Japan
[c] Central Institute for Experimental Animals, Kawasaki, Kanagawa 216-0001, Japan

ARTICLE INFO

Article history:
Received 15 May 2009
Received in revised form 3 August 2009
Accepted 29 October 2009
Available online xxx

Keywords:
HIV-1
Humanized mice
Immunopathogenesis

ABSTRACT

Creating a novel small animal model of HIV-1 infection that can support long-term systemic HIV-1 infection and produce HIV-1-specific immune response has a great benefit for studying HIV-1 pathogenesis *in vivo*. In the present study, we have generated a humanized mouse, NOG-hCD34 mouse, by transplanting newborn NOD/SCID/IL-2Rγ^{null} mice with human hematopoietic stem cells through hepatic injection. These mice were infected with a CCR5-tropic HIV-1 and were analyzed for plasma viral load, changes in peripheral blood T lymphocytes, and HIV-1-specific antibody production. High level of viral replication, increase in effector/memory CD8$^+$ T lymphocytes, class-switching to IgG, and production of HIV-1-specific IgGs were observed. Our findings suggest that NOG-hCD34 mice may have a wide variety of application in HIV-1 research.

1. Introduction

Human immunodeficiency virus type 1 (HIV-1) is a retrovirus that causes immunodeficiency exclusively in human [1]. The inability of HIV-1 to cause immunodeficiency in other animals has made authentic investigations in live animals extremely difficult, thus preventing the advancement of our understanding on the pathogenesis of HIV-1 *in vivo*.

Tremendous efforts have been made to generate a cost-efficient and readily accessible small animal model that can be used to investigate the pathogenesis of HIV-1, to test the effectiveness of anti-HIV-1 drug candidates, and to test HIV-1 vaccines *in vivo* [2–4]. Initial successful attempts included C.B17-severe combined immunodeficient (SCID) mice transplanted under the kidney capsule with fragments of human fetal thymus, lymph node, and human hematopoietic cells-containing human fetal liver (Thy/Liv SCID-hu mice) [5,6] or in the peritoneal space with human peripheral blood lymphocytes (hu-PBL-SCID mice) [7]. Thy/Liv SCID-hu mice are able to support *de novo* generation of human T lymphocytes and thus are useful for the studies of HIV-1 intrathymic infection and hematopoiesis suppression [8]. However, HIV-1 infection in Thy/Liv SCID-hu mice is restricted to the transplanted organ, and Thy/Liv SCID-hu mice are not able to support multilineage differentiation of human hematopoietic cells [9]. On the other hand, hu-PBL-SCID mice are able to reproduce high level of systemic HIV-1 infection, but the lack of on-going *de novo* human hematopoiesis and the short life span limited their application [10].

In order to improve a small animal model for the testing of anti-HIV-1 therapy and HIV-1 vaccines, HIV-1 infection must be sustained and immune response against HIV-1 must be generated within the animal. We have previously created a novel non-obese diabetic/severe combined immunodeficient (NOD/SCID) interleukin-2 receptor gamma chain (IL-2Rγ) knockout (NOD/SCID/IL-2Rγ^{null}; NOG) mouse strain, which lacks intrinsic T and B lymphocytes and functional natural killer cells [11]. NOG mice have been shown to be feasible for transplantation of human CD34$^+$ hematopoietic stem cells (hHSCs) and for supporting the differentiation of human T lymphocytes [11–13]. In adult NOG mice transplanted with hHSCs, it has been found that the CD34$^+$ cells successfully differentiated into human T and B lymphocytes, monocytes/macrophages, natural killer (NK) cells, as well as plasmacytoid and myeloid dendritic cells (DCs), and that these human cells were maintained for more than 150 days [12,14]. It was also reported that adult NOG mice transplanted with hHSCs supported HIV-1 infection for more than 3 months and produced HIV-1-specific antibodies [12]. These findings suggested that hHSCs-transplanted NOG mouse would be a useful animal model to study HIV-1 infection. However, whether hHSCs-transplanted NOG mice can mount a CD8$^+$ T lymphocyte-mediated immune response against HIV-1 has not been investigated yet.

In this paper, we generated humanized mice by transplanting newborn NOG mice with hHSCs via hepatic injection (NOG-hCD34 mice), because it has been suggested that transplantation of cord

* Corresponding author. Tel.: +81 75 751 4811.
E-mail address: ykoyanag@virus.kyoto-u.ac.jp (Y. Koyanagi).
[1] These authors contributed equally to this work.

0264-410X/$ – see front matter © 2009 Elsevier Ltd. All rights reserved.
doi:10.1016/j.vaccine.2009.10.154

blood (CB)-derived hHSCs into newborn mice results in better immune reconstitution [15,16]. Our humanized mice supported high level of HIV-1 replication. We observed that *de novo* generated $CD8^+$ T lymphocytes gained effector/memory phenotype in response to HIV-1 infection and massively proliferated. Based on our findings, we discuss the possibility of the application of NOG-CD34 mice, particularly those transplanted during the neonatal period, for HIV-1 research.

2. Material and methods

2.1. Mice

NOD/SCID/IL-2Rγ^{null} mice (NOG mice [11]) were obtained from the Central Institute for Experimental Animals (Kawasaki, Japan). The mice were maintained under specific pathogen-free conditions and were handled in accordance with the Regulation on Animal Experimentation at Kyoto University.

2.2. Purification and transplantation of CB-derived hHSCs

The purification and transplantation of CB-derived hHSCs was conducted as described previously with some modification [14–16]. Fresh human CB was obtained with parent written informed consent from healthy full-term newborns and CD34 MicroBead Kit (Miltenyi Biotec, Auburn, CA) was used according to the manufacturer's instructions. $CD34^+$ cells ($5–12 \times 10^4$) were intrahepatically injected into newborn mice of ages between 0 and 2 days after total radiation of 10 cGy per mouse in MBR-1520 X-ray irradiator (Hitachi Medico, Tokyo, Japan).

2.3. HIV-1 infection

~~NOG~~ mice were injected intraperitoneally with RPMI1640 or 1×10^5 50% tissue culture infective doses ($TCID_{50}$) of HIV-$1_{JR\text{-}CSF}$ [17] between 12 and 13 weeks post-transplantation. HIV-$1_{JR\text{-}CSF}$ solution was prepared and titrated previously described [18,19].

2.4. Quantification of HIV-1 RNA in plasma

The quantification of HIV-1 RNA in the plasma of the infected mice was routinely carried out using Amplicor HIV-1 monitor v1.5 according to the manufacturer's protocol (Roche Diagnostics, Mannheim, Germany).

2.5. Peripheral blood collection and isolation of nucleated cells from organs

Peripheral blood (PB) was routinely collected from NOG-hCD34 mice as described previously [16]. Red blood cells in the PB were lysed with 1× BD Lysis Buffer (BD Pharmingen, San Diego, CA). Mononuclear cells from bone marrow (BM), thymus, spleen, and lymph nodes were collected as described previously [16], and single cell suspensions were used for flow cytometric analysis or stored at −80 °C until use.

2.6. Flow cytometry

Flow cytometric analysis was performed with some modifications to the protocol previously described [15,19]. Following mouse monoclonal antibodies (mMAbs) and reagents were used: FITC-conjugated anti-CD19 (Dako, Tokyo, Japan), anti-CD8 (Dako), anti-CD4 (eBioscience, San Diego, CA), and anti-CD14 (Miltenyi Biotec) mMAbs, PE-conjugated anti-CD3 (Dako), anti-CD4 (Dako), anti-CCR5 (BD Pharmingen), and anti-CD34 (Miltenyi Biotec) mMAbs, biotinylated anti-CD45 (eBioscience) and anti-CD45RA (BD Pharmingen) mMAbs, PerCP-conjugated streptavidin (BD Immunocytometry systems, San Jose, CA), and FcR blocker (Miltenyi Biotec). Each antibody was controlled with appropriate isotype IgGs (Dako). Following first incubation, the cells were washed and further incubated with PerCP-conjugated streptavidin if needed. For p24 staining, the cells were permeabilized and fixed by treatment with BD Cytoperm/Cytofix solution (BD Pharmingen) and were stained with FITC-conjugated rat anti-HIV-1 p24 MAb (clone 2C2) [20] for 30 min at 4 °C in 1× BD PermWash buffer (BD Pharmingen). Data collection was performed on BD FACSCan (BD Biosciences, San Jose, CA), and the obtained data was analyzed with CellQuest software (BD Biosciences).

2.7. Detection of reactive human IgG against HIV-1 antigens

Plasma was collected from 1 mock-infected and 7 ~~HIV-1JR-CSF-infected~~ NOG-hCD34 mice upon the time of sacrifice. The presence of human IgGs against HIV-1 antigens in the collected plasma was examined by using a New Lav Blot 1 kit (Bio-Rad, Hercules, CA) according to the manufacturer's protocol.

2.8. Statistic analysis

Significant differences were determined by Student's *t* test or paired *t* test. *P* value less than 0.05 was considered significantly different.

3. Results

3.1. Reconstruction of human leukocytes in NOG-hCD34 mice

We first investigated the ability of newborn NOG mice transplanted with hHSCs to support human hematopoiesis. These mice are referred to as NOG-hCD34 mice. The flow cytometric analyses revealed that substantial percentages of human $CD45^+$ leukocytes including $CD3^+$ T lymphocytes and $CD19^+$ B lymphocytes already presented in the PB of 13-week-old mice and were stably maintained for at least 31 weeks (Table 1). $CD3^+$ T lymphocytes in the PB of these mice were singly positive for either CD4 or CD8 (Table 1). In the thymi of NOG-hCD34 mice, $CD45^+$ cells were detected in great abundance, which were predominantly CD4CD8 double positive cells (Table 1). In the BM sampled from femurs of NOG-hCD34 mice, we found large number of human $CD45^+$ leukocytes including $CD34^+$ hematopoietic cells, $CD3^+$ T lymphocytes, $CD19^+$ B lymphocytes, and $CD14^+$ monocytes (Table 1). In the secondary lymphoid organs of the mice, large populations of human leukocytes including $CD3^+$ and $CD19^+$ lymphocytes were detected (Table 1). In addition, we also found significant number of $CCR5^+CD4^+$ T lymphocytes, which are the target cells for CCR5-tropic HIV-1, in the spleen of NOG-hCD34 mice ($7.5 \pm 2.6\%$ in splenic mononuclear cells).

3.2. Significant and persistent viremia in PB of NOG-hCD34 mice

NOG-hCD34 mice between 12 and 13-week old were infected with HIV-$1_{JR\text{-}CSF}$ (1×10^5 $TCID_{50}$/mouse). HIV-$1_{JR\text{-}CSF}$ uses the chemokine receptor CCR5 as the co-receptor for its infection [21]. In the plasma of HIV-$1_{JR\text{-}CSF}$-infected NOG-hCD34 mice, high levels of HIV-1 were detected starting 2–3 weeks post-infection (wpi) ($1.28 \pm 0.65 \times 10^5$ copies/ml) and were maintained throughout the period of investigation (Fig. 1A). Of note, the plasma RNA levels were comparable to that found in patients with acute HIV-1 infection [22]. We also confirmed that HIV-1 RNA was undetectable in the plasma of mock-infected mice (<1600 copies/ml). In addition to the detection of viral RNA in plasma (Fig. 1A), we detected the cells positive for an HIV-1 antigen, p24, in the spleen of the infected mice

Please cite this article in press as: Sato K, et al. Dynamics of memory and naïve $CD8^+$ T lymphocytes in humanized NOD/SCID/IL-2Rγ^{null} mice infected with CCR5-tropic HIV-1. Vaccine (2009), doi:10.1016/j.vaccine.2009.10.154

Table 1
Reconstitution of human multilineage leukocytes in NOG-hCD34 mice[a,b].

Linage marker[c]	CD45+	CD3+	CD19+	CD4+	CD8+	CD14+	CD34+
PB (12–13-week old)	34.9 ± 11.3	10.2 ± 6.9	17.5 ± 6.3	4.7 ± 2.9	5.2 ± 3.3	n.a.[f]	n.a.
PB (28–31-week old)	33.3 ± 14.5	22.4 ± 6.8	8.7 ± 9.1	14.0 ± 6.2	5.4 ± 2.3	0.2 ± 0.2	n.a.
BM[d]	43.2 ± 20.8	7.8 ± 5.7	27.2 ± 24.6	n.a.	n.a.	2.7 ± 3.2	5.4 ± 3.9
Spleen[d]	75.9 ± 16.4	42.9 ± 22.9	25.6 ± 12.3	26.3 ± 10.6	11.5 ± 8.0	n.a.	n.a.
Lymph nodes[d]	94.8 ± 5.1	82.2 ± 8.7	8.0 ± 4.2	n.a.	n.a.	n.a.	n.a.

Linage marker[e]	CD45+	CD4SP	CD8SP	DP	DN
Thymus[d]	98.5 ± 0.4	12.6 ± 7.7	6.5 ± 4.9	76.3 ± 20.9	10.8 ± 10.6

[a] Each population of human leukocytes in NOG-hCD34 mice ($n = 4$–8) was analyzed by flow cytometry as described in Section 2.
[b] Average percentage of each linage marker positive cell in whole mononuclear cells is shown with standard deviation.
[c] Each linage marker indicates followings: CD45, pan leukocytes; CD3, T lymphocytes; CD19, B lymphocytes; CD14, monocytes; CD34, hematopoietic cells.
[d] Tissues were collected between 28 and 44 weeks old as described in Section 2.
[e] SP, single positive; DP, CD4CD8 double positive; DN, CD4CD8 double negative.
[f] Not analyzed.

(Fig. 1B). These results indicate that HIV-$1_{JR\text{-}CSF}$ was sufficiently replicated in NOG-hCD34 mice.

The PB samples of HIV-$1_{JR\text{-}CSF}$-infected and mock-infected NOG-hCD34 mice were periodically collected and human lymphocytes were sequentially analyzed by flow cytometry. We observed that peripheral CD4+ to CD8+ ratio of HIV-$1_{JR\text{-}CSF}$-infected mice was constantly lower than that of the mock-infected mice (Fig. 1C). Moreover, the percentage of peripheral CD4+ T lymphocytes in both

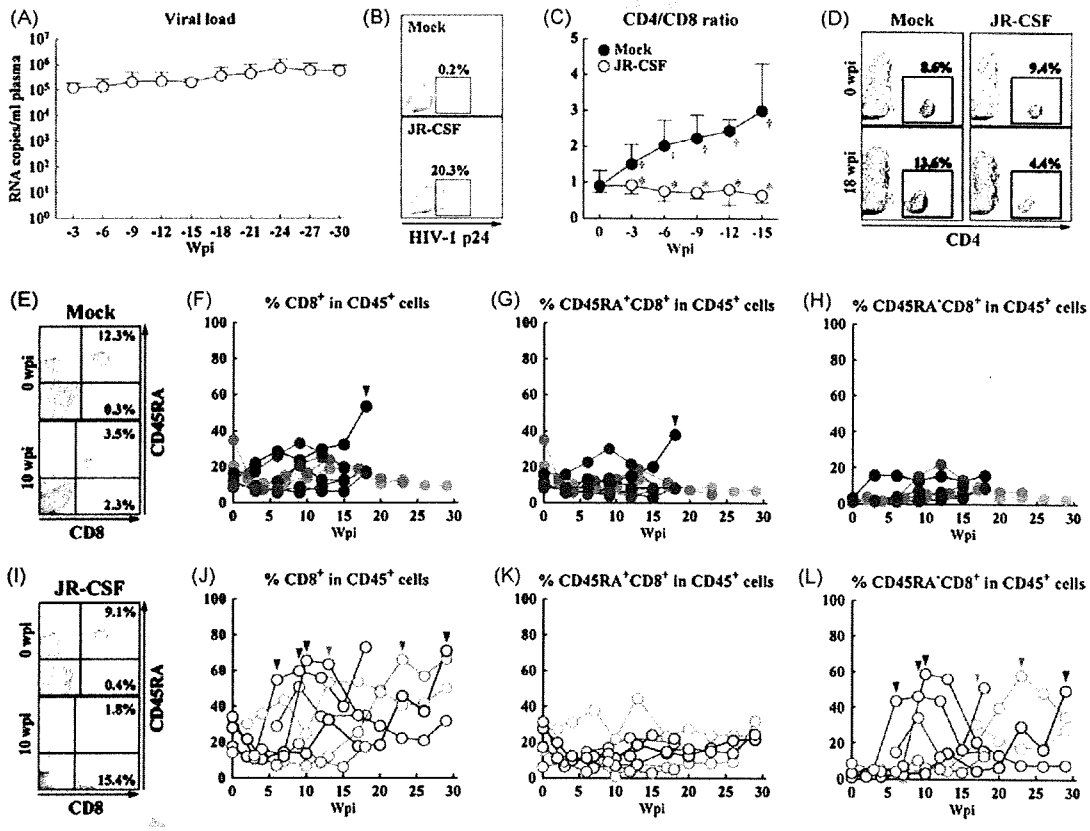

Fig. 1. Immunopathological analyses on CCR5-tropic HIV-1-infected NOG-hCD34 mice. NOG-hCD34 mice were intraperitoneally inoculated with ~~RPMI 1640~~ (for mock infection, filled circles, $n = 8$) or HIV-$1_{JR\text{-}CSF}$ (1×10^5 $TCID_{50}$/mouse, opened circles, $n = 7$) between 12 and 13-week old. (A) The longitudinal analysis on the plasma viral load of HIV-$1_{JR\text{-}CSF}$-infected mice. Plasma was routinely collected and HIV-1 RNA was quantified as described in Section 2. (B) Detection of HIV-1 antigen-expressing cells. Splenic mononuclear cells of mock-infected (top) and HIV-$1_{JR\text{-}CSF}$-infected (bottom) mice were stained with an anti-HIV-1 p24 antibody and analyzed by flow cytometry. A representative results are shown. The percentages in plots indicate the percentage of p24-positive cells in splenic whole mononuclear cells. (C–L) The longitudinal analyses in the PB of mock-infected and HIV-$1_{JR\text{-}CSF}$-infected mice. PB was routinely collected and longitudinally analyzed by flow cytometry. (C) CD4/CD8 ratio in the PB. Broken line in gray indicates CD4/CD8 ratio = 1. (D) Representative profiles of CD4+ T lymphocytes in the PB. The results in the PB of mock-infected (left) and HIV-$1_{JR\text{-}CSF}$-infected (right) mice at 0 wpi (top) and 18 wpi (bottom) are shown. The percentages in plots indicate the percentage of CD4-positive cells in whole mononuclear cells. (E–H) The percentages of whole CD8+ (F and J), naïve CD45RA+CD8+ (G and K), and memory CD45RA−CD8+ (H and L) T lymphocytes in the PB of mock-infected (E–H) and HIV-$1_{JR\text{-}CSF}$-infected (J–L) mice are shown. (E and I) Representative profiles of naïve and memory CD8+ T lymphocytes in the PB. The results in the PB of mock-infected (E) and HIV-$1_{JR\text{-}CSF}$-infected (I) mice at 0 wpi (top) and 10 wpi (bottom) are shown. The percentages in each quadrant indicate the percentages of CD8+CD45RA+ naïve cells (right upper) and CD8+CD45RA− memory cells (right lower) in whole mononuclear cells. In panels A and C, the data are assigned into periodic groups (0, 1–3, 4–6, 7–9, 10–12, 13–15, 16–18, 19–21, 22–24, 25–27, and 28–30 wpi). Error bars in panels A and C represent standard deviations. Arrowheads in panels F, G, J, and L indicate distinctive peaks or increases in the percentages of CD8+ T lymphocytes or their subsets. Asterisks represent statistical differences ($P < 0.05$ by Student's t test) versus the values of mock-infected mice at the same time point, and daggers represent statistical differences ($P < 0.05$ by paired t test) versus the value at 0 wpi.

Please cite this article in press as: Sato K, et al. Dynamics of memory and naïve CD8+ T lymphocytes in humanized NOD/SCID/IL-2Rγ^{null} mice infected with CCR5-tropic HIV-1. Vaccine (2009), doi:10.1016/j.vaccine.2009.10.154

human CD45$^+$ cells and whole mononuclear cells of mock-infected mice mildly increased, while this increase was not observed in HIV-$1_{JR\text{-}CSF}$-infected mice (Fig. 1D).

3.3. Proliferation of memory CD8$^+$ T lymphocytes in CCR5-tropic HIV-1-infected NOG-hCD34 mice

We also longitudinally analyzed on the percentages of CD8$^+$ T lymphocytes within human CD45$^+$ cells in the PB of mock-infected and HIV-$1_{JR\text{-}CSF}$-infected mice (Fig. 1E–I). CD8$^+$ T lymphocytes were further distinguished into memory and naïve populations on the basis of naïve T-cell marker CD45RA. In the mock-infected mice, the percentages of whole CD8$^+$ (Fig. 1F), CD45RA$^+$CD8$^+$ naïve (Fig. 1G), and memory CD45RA$^-$CD8$^+$ (Fig. 1H) T lymphocytes stayed consistent throughout the investigation with one exception that displayed increase in the percentage of CD8$^+$ T lymphocytes (Fig. 1F). This increase was attributed to an occasional increase in CD45RA$^+$ subset of CD8$^+$ T lymphocytes (Fig. 1G, arrowhead). In contrast, in 6 out of the 7 HIV-$1_{JR\text{-}CSF}$-infected mice, the percentages of whole CD8$^+$ and memory CD45RA$^-$CD8$^+$ T lymphocytes drastically increased after infection displaying distinctive peaks (Fig. 1J and L with arrowheads. A representative result is shown in Fig. 1I), while the percentages of naïve CD45RA$^+$CD8$^+$ T lymphocytes stayed quite stable (Fig. 1K). The peaks in the percentage of CD45RA$^-$CD8$^+$ T lymphocytes directly correlated to those in the percentage of CD8$^+$ T lymphocytes (Fig. 1J and L), indicating that the increase in the CD8$^+$ T lymphocyte population was caused by the increase in the CD45RA$^-$ memory subset.

3.4. Production of antibodies against HIV-1 antigens in CCR5-tropic HIV-1-infected NOG-hCD34 mice

In addition to the proliferative response of memory CD8$^+$ T lymphocytes in HIV-$1_{JR\text{-}CSF}$-infected mice, we found successful differentiation of human CD19$^+$ B lymphocytes in NOG-hCD34 mice (Table 1). To examine whether human antibody response against HIV-1 antigens was induced in the infected mice, we tested the plasma of a mock-infected and 7 HIV-$1_{JR\text{-}CSF}$-infected mice by Western blotting (Fig. 2), which has been clinically utilized for the definitive diagnosis of HIV-1 infection. In the plasma of all NOG-hCD34 mice, human IgG was detected (Fig. 2, lanes 2–4 and not shown), indicating that class-switching of immunoglobulin from IgM to IgG in human B cells occurred. However, we only detected human IgG that reacts with HIV-1 gp41 in the plasma of 2 infected mice (Fig. 2, lanes 3 and 4 with arrowheads). This suggests that generation of humoral immune response against HIV-1 may be limited in the infected mice.

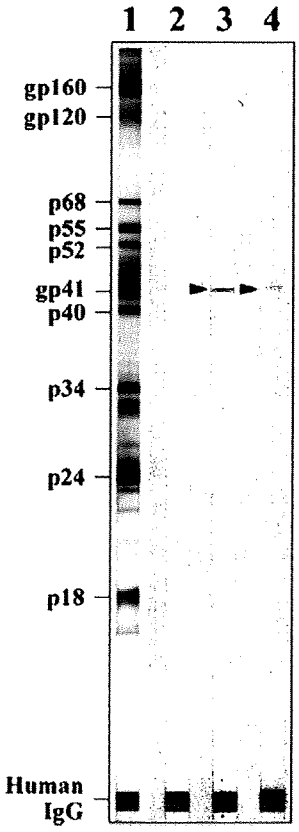

Fig. 2. Production of human IgG and antibodies against HIV-1 antigens in the plasma of CCR5-tropic HIV-1-infected NOG-hCD34 mice. Plasmas were collected from a mock-infected and 7 HIV-$1_{JR\text{-}CSF}$-infected NOG-hCD34 mice upon sacrifice and were examined for the presence of human IgG against HIV-1 antigens as described in Section 2. Representative results from serum of a human HIV-1 positive patient (positive control) (lane 1), and plasmas sampled from a mock-infected (lane 2) and 2 HIV-$1_{JR\text{-}CSF}$-infected (lanes 3 and 4) mice are shown. Arrowheads indicate bands showing the presence of human IgG that reacted with HIV-1 gp41.

4. Discussion

Adult NOG mice have been shown to be able to effectively support *de novo* generation of multilineage human immune cells when transplanted with hHSCs [11–13]. In the present study, we generated NOG-hCD34 mice, which are neonatal NOG mice transplanted with CB-derived hHSCs. These mice produced human T lymphocytes, B lymphocytes, and monocytes, and sustained steady human hematopoiesis for at least 31 weeks (217 days). They were susceptible to infection by HIV-$1_{JR\text{-}CSF}$, and showed high level of persistent viral replication. Furthermore, in addition to the production of HIV-1-specific IgG, human CD8$^+$ T lymphocytes proliferated in HIV-$1_{JR\text{-}CSF}$-infected mice. These suggest that NOG-hCD34 mice have the potential to be of valuable tool for the study of HIV-1 infection *in vivo*.

Classical xenotransplantation of hHSCs in mice used to be unsuccessful in producing *de novo* generated T lymphocytes, because immune cells in recipient mice interfered with hematopoiesis of the transplanted cells [23]. Human T lymphocytes failed to develop even in NOD/SCID mice, a strain of mice considered to have one of the most underdeveloped immune system [24]. The treatment of NOD/SCID mice with anti-NK cell antibody prior to xenotransplantation enhanced the engraftment efficiency, suggesting that NK cells were important mediators of graft failure in NOD/SCID mice [24]. Subsequently, highly immunodeficient strains of mice such as NOG mice and Rag2$^{-/-}\gamma c^{-/-}$ mice were generated and were found to be much better recipients for human grafts [11,15,25]. NOG mice, which are NOD/SCID mice with null mutation at the IL-2Rγ gene, were completely defective in NK cell function [11]. NOG-hCD34 mice supported the differentiation of human leukocytes including T lymphocytes from engrafted hHSCs, and they were shown to support long-term productive infection by HIV-1 [11–15]. In adult NOG mice transplanted with hHSCs, HIV-1 infection resulted in production of HIV-1-specific antibody response [12]. In our study, we transplanted CB-derived hHSCs into neonatal NOG mice by hepatic injection. Neonatal mice are thought to be better recipients for CB-derived hHSCs transplantation with regard to both engraftment and immune reconstitution as compared to their adult counterpart [15,16]. Indeed, like adult NOG mice transplanted with hHSCs, hHSCs in our NOG-hCD34 mice differentiated into mature T lymphocytes, B lymphocytes, monocytes, and DCs (Table 1 and not shown). High level of HIV-1 viremia (Fig. 1A) and HIV-1 antigen-expressing cells (Fig. 1B) were detected in these mice when they were infected with HIV-$1_{JR\text{-}CSF}$. The extent of human immune

Please cite this article in press as: Sato K, et al. Dynamics of memory and naïve CD8$^+$ T lymphocytes in humanized NOD/SCID/IL-2Rγ^{null} mice infected with CCR5-tropic HIV-1. Vaccine (2009), doi:10.1016/j.vaccine.2009.10.154

cell reconstitution, the duration in which the human cells were maintained, and the level of HIV-1 replication were comparable to those observed in the hHSCs-transplanted adult NOG mice [12,13] and hHSCs-transplanted Rag2$^{-/-}\gamma_c^{-/-}$ mice [16]. Class-switching of antibodies and the production of HIV-1-specific IgG were also observed in NOG-hCD34 mice (Fig. 2), as were observed in hHSCs-transplanted adult NOG mice [12]. Moreover, effector/memory CD8$^+$ T lymphocytes proliferated in response to HIV-1 infection (Fig. 1E–L). These data indicate that NOG-hCD34 mice have strong potential as an animal model for HIV-1 infection.

In both humans and mice, ~~T cell~~ precursors are selected in the thymus by thymic epithelial cells and DCs expressing major histocompatibility complexes (MHCs). Previous studies [26] and our findings shown in Table 1 strongly indicate that the human ~~T cells~~ are selected and maturated in the murine thymus as normal T lymphocytes need to recognize MHC molecules presented in the thymus to survive [27]. However, it is still uncertain how human T lymphocytes are selected in the recipient murine thymus by murine MHC molecules. It has been shown that mature T lymphocytes can develop from CB-derived mononuclear cell cultures with supplementation of stem cell factor and interleukin-7 but without thymic feeder cells *in vitro* [28], suggesting that development of human T lymphocytes in humanized mice may be independent of murine MHC molecules. On the other hand, others asserted that murine thymus can support human ~~T cell~~ differentiation via murine MHCs [29,30]. Although it is unclear whether human T lymphocytes *de novo* generated in hHSCs-xenotransplanted humanized mice are selected by human or murine MHCs, it has been reported that T lymphocytes capable of eliciting immune responses can be produced within humanized mice [14,16,23]. For instance, two reports showed that human CD8$^+$ T lymphocytes in the humanized mice infected with Epstein–Barr virus (EBV) massively proliferated, and that the CD8$^+$ T lymphocytes were reactivated *in vitro* by EBV antigens presented on human MHCs to some extent [16,31]. We have also observed the activation and the proliferation of human CD8$^+$ T lymphocytes in EBV-infected NOG-hCD34 mice (our unpublished observation). Although whether these CD8$^+$ ~~T cells~~ can elicit human MHC-restricted EBV-specific cytotoxic activity is still under investigation, these findings suggest that human CD8$^+$ T lymphocytes differentiated *de novo* in humanized mice may be selected and primed, at least partly, through human MHCs.

CD8$^+$ T lymphocytes can recognize viral peptides bound to MHC class I molecules and induce cytotoxicity against cells bearing the peptide/MHC class I complex, thus eliminating infected cells [32]. It is thought that CD8$^+$ T lymphocyte-mediated immune surveillance plays an important role in fighting against HIV-1 infection [33]. However, naïve CD8$^+$ T lymphocytes are not able to induce cytotoxicity and only become capable of cell killing after priming by antigen presenting cells (APCs) [34]. The priming of CD8$^+$ T lymphocytes requires complex interactions that include the ligation with both antigen peptide-loaded MHC class I and co-stimulatory molecules on APCs [34]. Successful priming of CD8$^+$ T lymphocytes lead to activation and proliferation of CD8$^+$ T lymphocytes, as well as down-regulation of surface CD45RA molecules [34,35]. The proliferation of CD8$^+$ T lymphocytes lacking CD45RA expression (effector/memory CD8$^+$ T lymphocytes) in HIV-1-infected humanized mice suggests that *de novo* generated leukocytes may be able to initiate and maintain HIV-1-specific CD8$^+$ T lymphocyte responses. Although the proliferation of effector/memory CD8$^+$ T lymphocytes was not associated with the reduction in plasma viral load, it is encouraging to know that such a CD8$^+$ T lymphocyte-mediated response against HIV-1 can be produced in hHSCs-transplanted NOG mice. As far as we know, the proliferation of effector/memory CD8$^+$ T lymphocytes in HIV-1 infection has not been reported in hHSCs-transplanted adult NOG mice [12,13], which may offer a broader application for NOG mice that receive neonatal transplantation. The generation of HIV-1-specific adaptive immune responses makes the present NOG-hCD34 mice system a possible candidate for HIV-1 vaccine evaluation.

Being able to allow HIV-1 replication makes hHSCs-transplanted NOG mice a good candidate for the evaluation of anti-HIV-1 drugs. However, it is not known whether hHSCs-transplanted NOG mice provided researchers with ideal system to study the interaction between human leukocytes and HIV-1. Both viral distraction of CD4$^+$ T lymphocytes and dysregulation of lymphocyte homeostasis are thought to contribute to immune deficiency caused by HIV-1 [36–38]. Therefore, it is important to study the effect of HIV-1 on different subsets of lymphocytes using NOG-hCD34 mice. We found that significant amount of both memory and naïve T lymphocytes were produced in NOG-hCD34 mice (data not shown). In addition, we also found that CCR5-tropic HIV-1 infection caused significant depletion of the memory but not the naïve subset of CD4$^+$ T lymphocytes in the periphery, which resulted in the reduction in overall CD4$^+$ T lymphocytes (Fig. 1C and D) (Nie et al., unpublished data). Furthermore, we found that CD4$^+$ T lymphocytes bearing CCR5 were severely reduced in the spleen of HIV-1-infected mice (Nie et al., unpublished data). These suggest that NOG-hCD34 mice can be used to study the dysregulation of CD4$^+$ T lymphocyte homeostasis after ~~HIV infection~~.

The emergence of severely immunodeficient mice, such as NOG mice and Rag2$^{-/-}\gamma_c^{-/-}$ mice, which can produce human T lymphocytes upon hHSCs transplantation, has made more sophisticated *in vivo* analyses on HIV-1 infection possible. However, the potential of these models to simulate HIV-1 infection and anti-HIV-1 immune response in human is to be explored in detail. Future investigations should include more thorough analyses on *de novo* reconstituted human immune system and how it is altered by HIV-1 infection, so that we can fully utilize this valuable tool.

Acknowledgements

We would like to thank Hiroko Kitayama (Institute for Virus Research, Kyoto University), Hisanori Fujino, Hidefumi Hiramatsu, Toshio Heike, and Tatsutoshi Nakahata (Graduate School of Medicine, Kyoto University) for helping our study. We also would like to express our appreciation for Ms. Kotubu Misawa's dedicated support. This work was supported by Grant-in-Aid for Scientific Research on Priority Areas from the Ministry of Education, Culture, Sports, Sciences, and Technology of Japan, and a Health and Labor Science Research Grant (Research on Publicly Essential Drugs and Medical Devices) from the Ministry of Health, Labor and Welfare of Japan and Japan Human Science Foundation. K.S. was supported by Research Fellowships of the Japan Society for the Promotion of Science for Young Scientists. Y.K. was supported by a grant from the Naito Foundation.

References

[1] Fauci AS. The human immunodeficiency virus: infectivity and mechanisms of pathogenesis. Science 1988;239(4840):617–22.
[2] Jamieson BD, Zack JA. Murine models for HIV disease. AIDS 1999;13(Suppl. A):S5–11.
[3] van Maanen M, Sutton RE. Rodent models for HIV-1 infection and disease. Curr HIV Res 2003;1(1):121–30.
[4] McCune J, Kaneshima H, Krowka J, Namikawa R, Outzen H, Peault B, et al. The SCID-hu mouse: a small animal model for HIV infection and pathogenesis. Annu Rev Immunol 1991;9:399–429.
[5] Namikawa R, Kaneshima H, Lieberman M, Weissman IL, McCune JM. Infection of the SCID-hu mouse by HIV-1. Science 1988;242(4886):1684–6.
[6] Kaneshima H, Shih CC, Namikawa R, Rabin L, Outzen H, Machado SG, et al. Human immunodeficiency virus infection of human lymph nodes in the SCID-hu mouse. Proc Natl Acad Sci USA 1991;88(10):4523–7.
[7] Mosier DE, Gulizia RJ, Baird SM, Wilson DB, Spector DH, Spector SA. Human immunodeficiency virus infection of human-PBL-SCID mice. Science 1991;251(4995):791–4.

Please cite this article in press as: Sato K, et al. Dynamics of memory and naïve CD8$^+$ T lymphocytes in humanized NOD/SCID/IL-2Rγ^{null} mice infected with CCR5-tropic HIV-1. Vaccine (2009), doi:10.1016/j.vaccine.2009.10.154

[8] Jenkins M, Hanley MB, Moreno MB, Wieder E, McCune JM. Human immunodeficiency virus-1 infection interrupts thymopoiesis and multilineage hematopoiesis *in vivo*. Blood 1998;91(8):2672–8.
[9] Berkowitz RD, Alexander S, Bare C, Linquist-Stepps V, Bogan M, Moreno ME, et al. CCR5- and CXCR4-utilizing strains of human immunodeficiency virus type 1 exhibit differential tropism and pathogenesis *in vivo*. J Virol 1998;72(12):10108–17.
[10] Fais S, Lapenta C, Santini SM, Spada M, Parlato S, Logozzi M, et al. Human immunodeficiency virus type 1 strains R5 and X4 induce different pathogenic effects in hu-PBL-SCID mice, depending on the state of activation/differentiation of human target cells at the time of primary infection. J Virol 1999;73(8):6453–9.
[11] Ito M, Hiramatsu H, Kobayashi K, Suzue K, Kawahata M, Hioki K, et al. NOD/SCID/γ_c^{null} mouse: an excellent recipient mouse model for engraftment of human cells. Blood 2002;100(9):3175–82.
[12] Watanabe S, Terashima K, Ohta S, Horibata S, Yajima M, Shiozawa Y, et al. hematopoietic stem cell-engrafted NOD/SCID/IL2Rγ^{null} mice develop human lymphoid system and induce long-lasting HIV-1 infection with specific humoral immune responses. Blood 2007;109(1):212–8.
[13] Watanabe S, Ohta S, Yajima M, Terashima K, Ito M, Mugishima H, et al. Humanized NOD/SCID/IL2Rγ^{null} mice transplanted with hematopoietic stem cells under nonmyeloablative conditions show prolonged life spans and allow detailed analysis of human immunodeficiency virus type 1 pathogenesis. J Virol 2007;81(23):13259–64.
[14] Hiramatsu H, Nishikomori R, Heike T, Ito M, Kobayashi K, Katamura K, et al. Complete reconstitution of human lymphocytes from cord blood CD34$^+$ cells using the NOD/SCID/γ_c^{null} mice model. Blood 2003;102(3):873–80.
[15] Ishikawa F, Yasukawa M, Lyons B, Yoshida S, Miyamoto T, Yoshimoto G, et al. Development of functional human blood and immune systems in NOD/SCID/IL2 receptor γ chain^{null} mice. Blood 2005;106(5):1565–73.
[16] Traggiai E, Chicha L, Mazzucchelli L, Bronz L, Piffaretti JC, Lanzavecchia A, et al. Development of a human adaptive immune system in cord blood cell-transplanted mice. Science 2004;304(5667):104–7.
[17] Koyanagi Y, Miles S, Mitsuyasu RT, Merrill JE, Vinters HV, Chen IS. Dual infection of the central nervous system by AIDS viruses with distinct cellular tropisms. Science 1987;236(4803):819–22.
[18] Koyanagi Y, Tanaka Y, Kira J, Ito M, Hioki K, Misawa N, et al. Primary human immunodeficiency virus type 1 viremia and central nervous system invasion in a novel hu-PBL-immunodeficient mouse strain. J Virol 1997;71(3):2417–24.
[19] Sato K, Aoki J, Misawa N, Daikoku E, Sano K, Tanaka Y, et al. Modulation of human immunodeficiency virus type 1 infectivity through incorporation of tetraspanin proteins. J Virol 2008;82(2):1021–33.
[20] Okuma K, Tanaka R, Ogura T, Ito M, Kumakura S, Yanaka M, et al. Interleukin-4-transgenic hu-PBL-SCID mice: a model for the screening of antiviral drugs and immunotherapeutic agents against X4 HIV-1 viruses. J Infect Dis 2008;197(1):134–41.
[21] Dejucq N, Simmons G, Clapham PR. Expanded tropism of primary human immunodeficiency virus type 1 R5 strains to CD4$^+$ T-cell lines determined by the capacity to exploit low concentrations of CCR5. J Virol 1999;73(9):7842–7.
[22] Hockett RD, Kilby JM, Derdeyn CA, Saag MS, Sillers M, Squires K, et al. Constant mean viral copy number per infected cell in tissues regardless of high, low, or undetectable plasma HIV RNA. J Exp Med 1999;189(10):1545–54.
[23] Legrand N, Weijer K, Spits H. Experimental models to study development and function of the human immune system *in vivo*. J Immunol 2006;176(4):2053–8.
[24] Kerre TC, De Smet G, De Smedt M, Zippelius A, Pittet MJ, Langerak AW, et al. Adapted NOD/SCID model supports development of phenotypically and functionally mature T cells from human umbilical cord blood CD34$^+$ cells. Blood 2002;99(5):1620–6.
[25] Gimeno R, Weijer K, Voordouw A, Uittenbogaart CH, Legrand N, Alves NL, et al. Monitoring the effect of gene silencing by RNA interference in human CD34$^+$ cells injected into newborn RAG2$^{-/-}\gamma_c^{-/-}$ mice: functional inactivation of p53 in developing T cells. Blood 2004;104(13):3886–93.
[26] Macchiarini F, Manz MG, Palucka AK, Shultz LD. Humanized mice: are we there yet? J Exp Med 2005;202(10):1307–11.
[27] Liu YJ. A unified theory of central tolerance in the thymus. Trends Immunol 2006;27(5):215–21.
[28] Sanchez M, Alfani E, Visconti G, Passarelli AM, Migliaccio AR, Migliaccio G. Thymus-independent T-cell differentiation *in vitro*. Br J Haematol 1998;103(4):1198–205.
[29] Robin C, Bennaceur-Griscelli A, Louache F, Vainchenker W, Coulombel L. Identification of human T-lymphoid progenitor cells in CD34$^+$ CD38^{low} and CD34$^+$ CD38$^+$ subsets of human cord blood and bone marrow cells using NOD-SCID fetal thymus organ cultures. Br J Haematol 1999;104(4):809–19.
[30] Weekx SF, Snoeck HW, Offner F, De Smedt M, Van Bockstaele DR, Nijs G, et al. Generation of T cells from adult human hematopoietic stem cells and progenitors in a fetal thymic organ culture system: stimulation by tumor necrosis factor-α. Blood 2000;95(9):2806–12.
[31] Yajima M, Imadome KI, Nakagawa A, Watanabe S, Terashima K, Nakamura H, et al. A new humanized mouse model of Epstein-Barr virus infection that reproduces persistent infection, lymphoproliferative disorder, and cell-mediated and humoral immune responses. J Infect Dis 2008;198(5):673–82.
[32] Hislop AD, Taylor GS, Sauce D, Rickinson AB. Cellular responses to viral infection in humans: lessons from Epstein-Barr virus. Annu Rev Immunol 2007;25:587–617.
[33] Vasan S, Schlesinger SJ, Arrode G. T cell immune responses to HIV-1. Front Biosci 2007;12:2330–43.
[34] Steinman RM. The dendritic cell system and its role in immunogenicity. Annu Rev Immunol 1991;9:271–96.
[35] Clement LT. Isoforms of the CD45 common leukocyte antigen family: markers for human T-cell differentiation. J Clin Immunol 1992;12(1):1–10.
[36] Centlivre M, Sala M, Wain-Hobson S, Berkhout B. In HIV-1 pathogenesis the die is cast during primary infection. AIDS 2007;21(1):1–11.
[37] Brenchley JM, Schacker TW, Ruff LE, Price DA, Taylor JH, Beilman GJ, et al. CD4$^+$ T cell depletion during all stages of HIV disease occurs predominantly in the gastrointestinal tract. J Exp Med 2004;200(6):749–59.
[38] Okoye A, Meier-Schellersheim M, Brenchley JM, Hagen SI, Walker JM, Rohankhedkar M, et al. Progressive CD4$^+$ central memory T cell decline results in CD4$^+$ effector memory insufficiency and overt disease in chronic SIV infection. J Exp Med 2007;204(9):2171–85.

Please cite this article in press as: Sato K, et al. Dynamics of memory and naïve CD8$^+$ T lymphocytes in humanized NOD/SCID/IL-2Rγ^{null} mice infected with CCR5-tropic HIV-1. Vaccine (2009), doi:10.1016/j.vaccine.2009.10.154

Virology 386 (2009) 23–31

Contents lists available at ScienceDirect

Virology

journal homepage: www.elsevier.com/locate/yviro

Raft localization of CXCR4 is primarily required for X4-tropic human immunodeficiency virus type 1 infection

Haruka Kamiyama [a,b], Hiroaki Yoshii [a], Yuetsu Tanaka [c], Hironori Sato [a,d], Naoki Yamamoto [a,e], Yoshinao Kubo [a,*]

[a] Department of AIDS Research, Institute of Tropical Medicine, Nagasaki University, 1-12-4 Sakamoto, Nagasaki, Nagasaki 852-8523, Japan
[b] Department of Cellular Biochemistry, Graduate School of Human Health Science, Siebold University of Nagasaki, Nagayo, Nagasaki 851-2195, Japan
[c] Department of Immunology, Graduate School and Faculty of Medicine, University of the Ryukyus, Nishihara, Okinawa 903-0215, Japan
[d] Laboratory of Viral Genomics, Center for Pathogen Genomics, National Institute of Infectious Diseases, Gakuen 4-7-1, Musashimurayama-shi, Tokyo 208-0011, Japan
[e] AIDS Research Center, National Institute of Infectious Diseases, Shinjuku-ku, Tokyo 162-8640, Japan

ARTICLE INFO

Article history:
Received 3 June 2008
Returned to author for revision
10 November 2008
Accepted 17 December 2008

Keywords:
CD4-independent HIV-1
CXCR4
Raft

ABSTRACT

Human immunodeficiency virus type 1 (HIV-1) infection is initiated by successive interactions of viral envelope glycoprotein gp120 with two cellular surface proteins, CD4 and chemokine receptor. The two most common chemokine receptors that allow HIV-1 entry are the CCR5 and CXCR4. The CD4 and CCR5 are mainly localized to the particular plasma membrane microdomains, termed raft, which is rich in glycolipids and cholesterol. However, the CXCR4 is localized only partially to the raft region. Although the raft domain is suggested to participate in HIV-1 infection, its role in entry of CXCR4-tropic (X4-tropic) virus is still unclear. Here, we used a combination of CD4-independent infection system and cholesterol-depletion-inducing reagent, methyl-β-cyclodextrin (MβCD), to address the requirement of raft domain in the X4-tropic virus infection. Treatment of CD4-negative, CXCR4-positive human cells with MβCD inhibited CD4-independent infection of the X4-tropic strains. This inhibitory effect of the cholesterol depletion was observed even when the CXCR4 was over-expressed on the target cells. Soluble CD4-induced infection was also inhibited by MβCD. The MβCD had no effect on the levels of cell surface expression of CXCR4. In contrast to these infections, MβCD treatment did not inhibit CD4-dependent HIV-1 infection in the wild type CD4-expressing cells. This study and previous reports showing that CD4 mutants localized to non-raft domains function as HIV-1 receptor indicate that CXCR4 clustering in the raft microdomains, rather than CD4, is the key step for the HIV-1 entry.

Introduction

Human immunodeficiency virus type 1 (HIV-1) gains entry into susceptible cells by fusion of the viral membrane with the cell plasma membrane (Dimitrov, 2000). This process is generally initiated by the binding of the HIV-1 envelope (Env) glycoprotein gp120 to CD4 on the host cell surface. The binding then induces conformational change of the gp120, which allows gp120 to interact with a cellular surface chemokine receptor, termed coreceptor. HIV-1 can use many types of chemokine receptors for the entry (Shimizu et al., 2000). The two most common types of the coreceptors of the HIV-1 are the CC chemokine receptor 5 (CCR5) and the CXC chemokine receptor 4 (CXCR4) (Berger et al., 1999). Successive conformational changes in the gp120 during these interactions with cellular surface molecules render initially occluded hydrophobic domain of the envelope gp41 subunit available to fusion with cellular plasma membrane (Doms, 2000).

Clustering of multiple CD4 and coreceptor molecules at the site of the fusion is presumed to be necessary for the efficient fusion of the viral and host cell membranes (Kuhmann et al., 2000). Because both the gp120–CD4 and gp120–chemokine receptor associations are reversible, and because CD4 binding site of the gp120 is conformationally masked (Kwong et al., 2002), multiple CD4 and chemokine receptor molecules should almost simultaneously be gathered and interact with the multiple gp120 at the place of virus–host cell membrane fusion (Dimitrov 2000; Doms, 2000; Kwong et al., 2002).

Membrane microdomains or lipid rafts are regions of host cell membrane enriched in glycosphingolipids, sphingomyelin, cholesterol, glycophosphatidylinositol-anchored proteins, and signaling proteins (Simons and Ikonen, 1997). The rafts are thought to serve as sites for recruitment of gp120–gp41–CD4–coreceptor complexes in a limited area on the cell surface. Increasing evidence indicate such a scaffolding role of the rafts in HIV-1 entry; (i) HIV-1 infection is blocked by targeting CD4 to non-raft membrane domains (Del Real et al., 2002); (ii) membrane raft microdomains mediate lateral assemblies required for HIV-1 infection (Manes et al., 2000); (iii) HIV-1 gp120-induced co-clustering of CD4 and coreceptor into the raft

* Corresponding author. Fax: +81 95 819 7805.
E-mail address: yoshinao@net.nagasaki-u.ac.jp (Y. Kubo).

0042-6822/$ - see front matter © 2008 Elsevier Inc. All rights reserved.
doi:10.1016/j.virol.2008.12.033

domains is prevented by removal of cholesterol from cell plasma membrane and the depletion of cholesterol from target cells inhibits their susceptibility to HIV-1 infection (Manes et al., 2000; Popik et al., 2002; Liao et al., 2001; Viard et al., 2002). Together with other results, reported data are compatible with the possibility that the recruitment of gp120–gp41–CD4-coreceptor complexes into the raft domains is required for the HIV-1 infection (Liao et al., 2001; Manes et al., 2000; Popik et al., 2002). However, it is not clear what is the determinant for the recruitment of the complexes into raft domains.

CD4 (Millan et al., 1999; Manes et al., 2000; Del Real et al., 2002) and CCR5 (Nguyen and Taub, 2002b; Gaibelet et al., 2006) have been demonstrated to be present in lipid rafts, and to constitutively interact each other before the gp120 binding. In contrast, CXCR4 is localized only partially to the rafts, as evidenced with partial colocalization with GM1, a raft marker (Manes et al., 2000; Del Real et al., 2002; Nguyen and Taub, 2002a). It has been reported that a CD4 mutant, which is localized to non-raft domains of the plasma membrane, blocks HIV-1 entry, indicating that raft localization of CD4 is critical in HIV-1 infection (Del Real et al., 2002). However, more recent studies are consistent with a possibility that the raft localization of CD4 is not required for the virus entry (Popik and Alce, 2004; Percherancier et al., 2003), indicating that CD4 is not the determinant for clustering of gp120–gp41–CD4–chemokine receptor complexes into raft domains. Due to the initial localization of CXCR4 in the non-raft region and the inconsistencies in prior studies, a role of raft domains in CXCR4-tropic (X4-tropic) HIV-1 entry is not clear yet.

These apparently controversial observations prompted us to examine the possibility that recruitment of CXCR4 to raft microdomains, rather than CD4 raft localization, is the determinant for the clustering of gp120–gp41–CD4–CXCR4 complexes into raft domains. To test the possibility, we used HIV-1 pseudotype viruses that have the X4-tropic Env proteins and can establish infection of CXCR4-expressing cells without interaction with CD4 (CD4-independent infection). The viruses were used to infect cells whose cholesterol were depleted in advance with treatment by a cholesterol-solubilizing agent, methyl-β-cyclodextrin (MβCD) (Simons and Ikonen, 1997), and viral infectivity was measured. We further examined a role of raft localization of CXCR4 in the HIV-1 entry, as follows. The CD4-dependent infection induced by soluble CD4 was used to infect cholesterol-depleted cells. By this approach, we can determine if the raft localization of CXCR4 is essential in the HIV-1 infections, because these infections occur independently of CD4 raft localization. Our results are compatible with the working hypothesis described above and suggest a supportive role of CD4 in augmenting the raft recruitment/clustering of CXCR4.

Results

MβCD inhibits CD4-independent, CXCR4-dependent HIV-1 infection

To examine whether raft domain architectures are required for CD4-dependent and -independent entry of X4-tropic viruses, we used an infection system of pseudotyped viruses carrying Env proteins of X4-tropic HIV-1 strains, mNDK, or 8X, that allow both CD4-dependent and -independent infections in CD4-positive and -negative cells, respectively (Dumonceaux et al., 1998, Hoffman et al., 1999, Kubo et al., 2007). As targets of virus infections, we used human NP2 cells expressing both CD4 and CXCR4, or CXCR4 alone (Soda et al., 1999). The raft domain of target cells were depleted by the treatment with MβCD (Simons and Ikonen, 1997) and used for infections of the pseudotyped HIV-1 viruses. As a control of HIV-1 receptor independent infection, we used the VSV-G-pseudotyped HIV-1. Incubation with MβCD did not suppress but rather increased the VSV-G-pseudotyped virus infection (Fig. 1A). This MβCD treatment (1 and 5 mM) did not affect cell growth (data not shown).

Notably, transduction titers of the HIV-1 vectors having the CD4-independent Env proteins (mNDK and 8X) were reduced to about 25% by the increasing concentrations of MβCD treatments of the CD4-negative, CXCR4-positive cells (Fig. 1B, gray bars, NP2/X4 cells). In contrast, inhibitory effects of MβCD were less prominent in the CD4-dependent infections of the same viruses: transduction titers of the HIV-1 vectors were reduced to about 75% at 5 mM of MβCD (Fig. 1B, open bars, NP2/CD4/X4 cells). Transduction titer of the HIV-1 vector having Env protein of the NDK HIV-1 strain, the CD4-dependent parental strain of the mNDK variant, was not significantly inhibited by MβCD (Fig. 1C). These results show that MβCD inhibits CXCR4-mediated infection but co-expression of CD4 counteracts the inhibitory effects. When excess of cholesterol was added, the inhibitory effect of MβCD on the CD4-independent infection was abrogated (Fig. 1D), confirming that cholesterol extraction is a primary cause of suppression of the CD4-independent infection by MβCD.

To assess if the MβCD treatment indeed had depleted cholesterol from target cell membranes, cells were stained with the cholesterol-binding agent, filipin. Binding of filipin to cholesterol decreases filipin fluorescence at 525 nm (Severs and Robenek, 1983; Castanho et al., 1992). Fluorescence strength of filipin in the MβCD-treated cells was reproductively increased compared to that of the untreated control cells (Fig. 1E). The results indicate that cholesterol of cell membrane was indeed extracted by MβCD treatment in our experimental system.

Over-expression of CXCR4 does not affect the inhibitory effect of MβCD on CD4-independent HIV-1 infection

In our CD4-independent infection system, virus enters into cells using endogeneously expressed CXCR4. To know whether MβCD still inhibits infection when cells express exogenously abundant amounts of CXCR4, human 293T and TE671 cells were transduced by an HA-tagged CXCR4 encoding murine leukemia virus vector (Kubo et al., 2003). Over-expression of CXCR4 in the transduced cells was observed by flow cytometry analysis (Fig. 2A). Transduction titers of the CD4-independent mNDK vector in the CXCR4-over-expressing cells increased about 3 to 4 times compared to those in the original cells (Fig. 2B). This result indicates that CXCR4-over-expression increases the susceptibility to CD4-independent infection.

Effect of CXCR4-over-expression on the inhibition of CD4-independent infection by MβCD was analyzed. The MβCD treatment suppressed the CD4-independent infection in the CXCR4-over-expressing cells, as it did in the original cells (Fig. 3, upper 4 panels). However, exogenous introduction of CD4 into the target cells abrogated the inhibitory effect of MβCD on the HIV-1 infection (Fig. 3 lower panel), as reported (Viard et al., 2002). The results indicate that maintenance of the raft domain architectures on the plasma membrane of the target cells are absolutely required for the CD4-independent infection and suggest that the raft localization of CXCR4 is important for the HIV-1 entry. The treatment with MβCD alone or MβCD plus cholesterol occasionally conferred transduction titers of the VSV-G and mNDK vectors higher (Figs. 1A, D, and 3). The mechanism was not understood.

MβCD treatment inhibits CD4-independent HIV-1 Env-mediated cell-cell fusion

The above result showed that the depletion of cholesterol by MβCD inhibited the HIV-1 Env-mediated infection. To examine if the depletion of cholesterol affects the HIV-1 Env-mediated cell-cell fusion, Env expression plasmid-transfected effector cells and LTR-LacZ-transfected target cells were co-cultured (see Materials and methods). The target cells were co-transfected with the Tat expression and LTR-LacZ plasmids, and then were treated with MβCD. LacZ activities of the cells were comparable between the cells with and without

the MβCD treatment (data not shown), indicating that the MβCD treatment does not affect LacZ functional expression. In NP2/CD4/X4 cells, the mNDK Env-mediated cell-cell fusion was not significantly inhibited by MβCD (Fig. 4, NP2/CD4/X4). On the other hand, in CD4-negative NP2/X4, TE671, and 293T cells, the CD4-independent mNDK Env-mediated cell–cell fusion was inhibited to 40 to 60% of that in the untreated cells (Fig. 4, NP2/X4, TE671, and 293 T). The results are consistent with previous study (Ablan et al., 2006). The cell–cell fusion activity inhibited by MβCD was recovered, when excess of cholesterol was added into the culture (Fig. 4, MβCD+chol). The results were compatible with those of cell-free virus infection (Figs. 1 and 3). Taken together, our results suggest that cholesterol in the cell membrane played an important role in the CD4-independent HIV-1 Env-induced cell–cell fusion and virus entry.

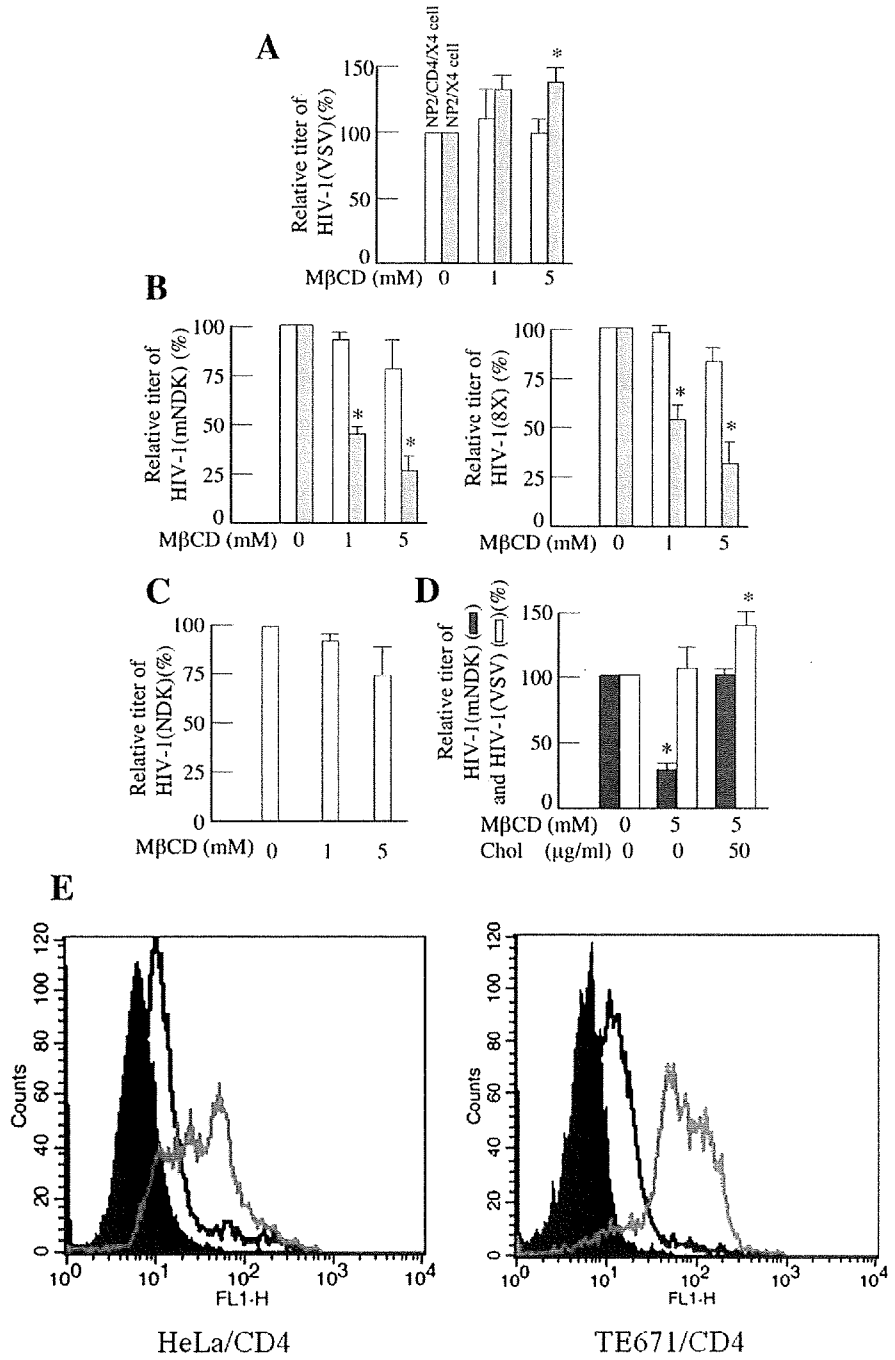

Fig. 1. Effects of MβCD on HIV-1 infection by different Env protein. (A) Effects of MβCD on VSV-G-pseudotyped vector infection in NP2 cells expressing CXCR4 alone (NP2/X4) or both of CXCR4 and CD4 (NP2/CD4/X4). Cells were treated with 0, 1, 5 mM MβCD for 30 min at 37 °C. (B) Effects of MβCD on CD4-independent mNDK Env-pseudotyped HIV-1 vector infection in NP2/X4 and NP2/CD4/X4 cells. Cells were treated with 0, 1, 5 mM MβCD for 30 min at 37 °C. (C) Effects of MβCD on the CD4-dependent NDK-pseudotyped vector in NP2/CD4/X4 cells. (D) Abrogation of MβCD inhibitory effects on mNDK vector infection by cholesterol. The cells were pre-treated for 30 min at 37 °C as indicated. Relative transduction titers to those in untreated cells are indicated. This experiment was repeated three times and results are shown as means+SD. Asterisks indicate statistically significant differences compared to their controls. (E) Cholesterol levels in HeLa/CD4 or TE671/CD4 cells after MβCD treatment. MβCD-treated cells were stained with filipin, and fluorescence strength at 525 nm was analyzed by a flow cytometer. Closed area indicates cells unstained with filipin as a negative control. Open area indicates MβCD-untreated and filipin-stained cells. Gray lines indicate MβCD-treated and filipin-stained cells.

To assess the possibility that MβCD altered the CXCR4 expression, expression levels of CXCR4 in the treated cells were analyzed by a flow cytometer. Treatment of MβCD did not affect the expression of CXCR4 in NP2/X4, 293 T, and TE671 cells (Fig. 5). This result indicates that the inhibition of CD4-independent infection by MβCD is not induced by reducing CXCR4 expression.

Localization of CXCR4 in rafts

The classical way to examine the raft association of membrane proteins includes treatment of cells with Triton X-100 followed by Western blot analysis of soluble and insoluble fractions. The fractions that are not solubilized by Triton X-100 are defined as the raft membrane domains (Simons and Ikonen, 1997). Using this approach, we examined localization of CXCR4 in the raft domains in the presence or absence of MβCD. We also examined raft localization of CD4 as a maker of raft protein (Manes et al., 2000; Del Real et al., 2002; Percherancier et al., 2003; Popik and Alce, 2004). CD4 levels in the insoluble fraction were higher than that in the soluble fraction in all cells examined (Fig. 6A), suggesting that raft domains were correctly separated by this protocol. In contrast to CD4, CXCR4 levels in the insoluble fractions of NP2 and TE671 cells were lower than those in the soluble fractions. In contrast to these cells, CXCR4 was detected in the insoluble fraction of 293T cells. CXCR4 was detected in both of soluble and insoluble fractions after treatment of 293T cells with MβCD (Fig. 6A), suggesting that CXCR4 is partially transferred to non-raft domains from raft domains by the MβCD treatment in 293T cells. However, the transfer of CXCR4 to non-raft domains by the MβCD treatment in NP2 and TE671 cells was not observed, because majority of CXCR4 molecules were originally localized to the non-raft domains in the cells.

To further assess the localization of CXCR4 in the plasma membrane, confocal laser scanning microscopy using the anti-CXCR4 antibody and CT-B was performed. In almost all 293T cells examined, CXCR4 was co-localized with CT-B, indicating that CXCR4 is largely localized to the raft domains in the MβCD-untreated 293T cells (Fig. 6B, the most upper panels). However, the fluorescent signals of the CXCR4 and CT-B were not matched in about 5% of MβCD-treated 293 T cells (Fig. 6B, the second panels). The data indicate that CXCR4 is partially transferred to non-raft domains by the MβCD treatment.

In contrast to the 293 T cells, the individual dot signals of CXCR4 were not completely matched to those of CT-B in the almost all TE671 cells (Fig. 6B, third panel, and arrows in the bottom panel). Interestingly, when two or more cells came in contact, CXCR4 molecules at cell–cell adhesion site appeared to be colocalized with CT-B (Fig. 6B bottom panel). The result may imply clustering of CXCR4 into raft domains at the

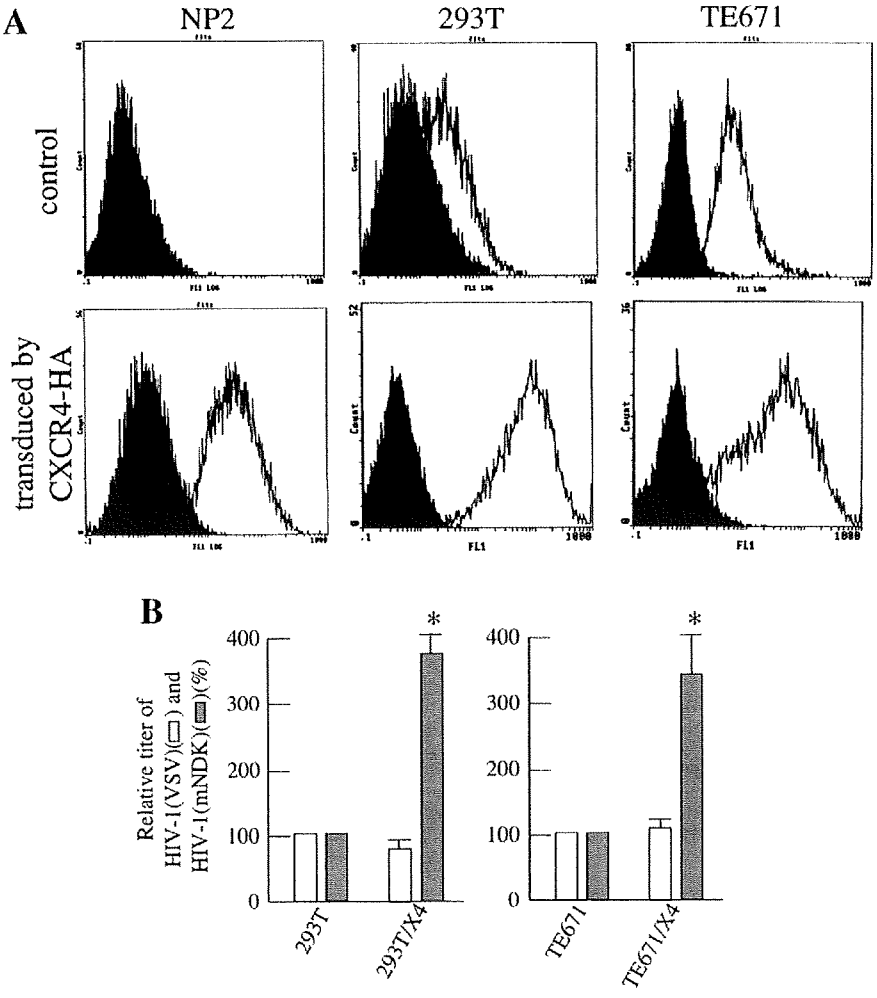

Fig. 2. Effect of CXCR4 overexpression on mNDK HIV-1 vector infection. (A) Cell-surface expression of CXCR4 in original NP2, 293 T, and TE671 cells and their CXCR4-overexpressing cells was analyzed by a flow cytometer using the anti-CXCR4 antibody (A80). Closed and open areas indicate the cells that were incubated in the absence and presence of the A80 antibody, respectively. (B) Relative transduction titers of the VSV-G (open bar) and mNDK (closed bar) vectors in the CXCR4-overexpressing cells to those in the original cells are indicated. This experiment was repeated three times and results are shown as means+SD. Asterisks indicate statistically significant differences compared to their controls.

cell–cell contact site, and is compatible with previous observations that contact between HIV-1 Env-expressing and receptor-expressing cells can induce translocation of CXCR4 from non-raft to raft regions (Manes et al., 2000; Nguyen et al., 2005), although the CXCR4 localization to raft domains at cell–cell contact site was independent of HIV-1 Env in our study. Raft localization of CXCR4 in NP2 cells could not be analyzed, because CT-B did not bind to NP2 cells. These results of cell-staining studies with the 293 T and TE671 cells were consistent with the results of cell fractionation studies of Fig. 6A.

MβCD inhibits soluble CD4-induced CD4-dependent infection

The MβCD treatment significantly inhibited the CD4-independent HIV-1 infection, but did not the CD4-dependent infection in the cells exogenously expressing CD4. To know whether the CD4-dependent infection does not require raft microdomains of the target cells, effect of MβCD on soluble CD4 (sCD4)-induced CD4-dependent infection was analyzed. In this experiment, CD4-dependent infection occurs independently of CD4 localization to raft domains. Interestingly, the MβCD treatment significantly inhibited the sCD4-dependent vector (NDK and HXB2) infection (Fig. 7), indicating that sCD4-induced CD4-dependent infection requires the raft membrane domains of the target cells. The result is compatible with the previous report that HIV-1 infection is inhibited by MβCD in cells expressing a CD4 mutant that is localized to non-raft domains (Popik and Alce, 2004).

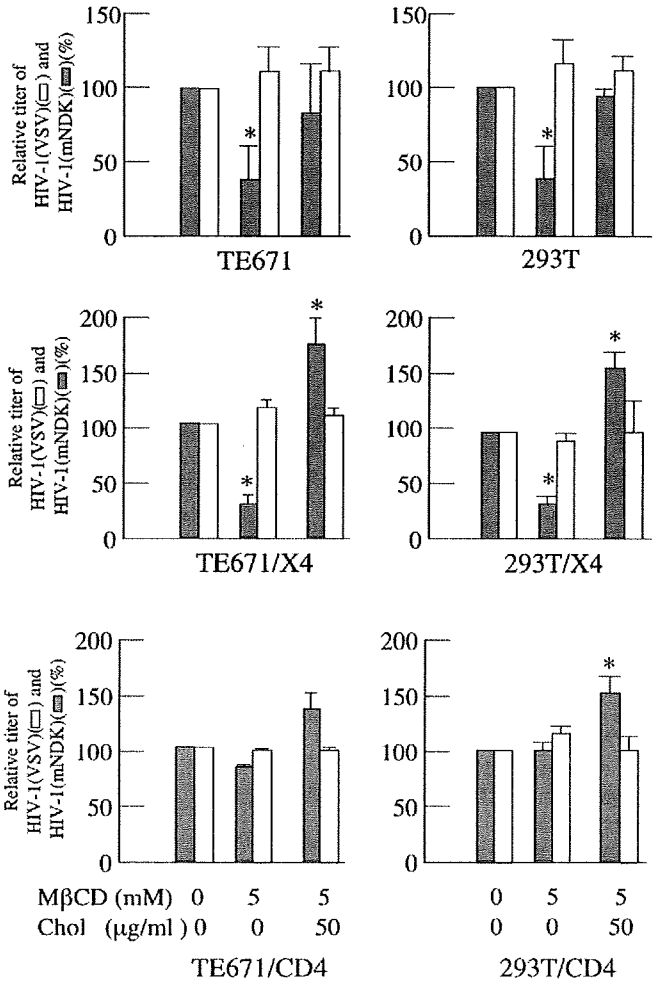

Fig. 3. Effects of MβCD on mNDK HIV-1 vector infection in CXCR4-overexpressing TE671 and 293T cells. Relative transduction titers of the VSV-G (open bar) and mNDK (closed bar) vectors in MβCD-treated, CXCR4-overexpressing TE671 and 293 T cells to those in untreated cells are indicated. Cells were treated with 0, 1, 5 mM MβCD for 30 min at 37 °C. Relative transduction titers to those in untreated cells are indicated. This experiment was repeated three times and results are shown as means+SD. Asterisks indicate statistically significant differences compared to their controls.

Discussion

The raft domains are thought to participate in versatile biological events, such as signal transductions and cell–cell communications, as a scaffold for clustering particular membrane proteins. In this study, we examined potential roles of the raft in the X4-tropic HIV-1 infections. Previous puzzling observations (Del Real et al., 2002, Popik and Alce, 2004; Percherancier et al., 2003) prompted us to examine the possibility that raft localization of CXCR4 rather than CD4 is primarily required for X4-tropic HIV-1 infection. To avoid complications of CD4-dependent infection system, we used CD4-independent or sCD4-induced HIV-1 infection systems.

CD4-independent variants are thought to be prototypes of CD4-dependent variants, and to show fundamental entry pathway shared by both CD4-dependent and -independent viruses (Paolo, 2006; Kubo et al., 2007). Because the CD4-independent and sCD4-induced HIV-1 infections occur independently of CD4 raft localization, they are useful to study the function of CXCR4 raft localization in HIV-1 infection. The MβCD treatment significantly inhibited the CD4-independent (Fig. 1) and sCD4-induced CD4-dependent HIV-1 infections (Fig. 7). In addition, the CXCR4 over-expression did not affect the sensitivity of CD4-independent infection to the MβCD treatment (Fig. 3). These results indicate that raft localization of CXCR4 is required for these HIV-1 infections.

CXCR4 molecules were localized in the raft domains at cell–cell contact regions, but did not at exposed membrane regions (Fig. 6). The HIV-1 vector particles should bind to the CXCR4 molecules in the exposed cell surface regions, in which CXCR4 is localized to non-raft domains. How do the CXCR4 molecules present in non-raft domains function for the X4-tropic HIV-1 infection? It has been already reported that CXCR4 clusters to raft domains after HIV-1 binding to the cell surface receptors (Manes et al., 2000; Sorice et al., 2001; Del Real et al., 2002; Nguyen et al., 2005). Therefore, after the CD4-independent virus binds to CXCR4 in non-raft domains, the complexes could move and cluster in the raft domains and induce membrane fusion for the subsequent viral entry. Alternatively, binding of the CD4-independent HIV-1 to CXCR4 present in the raft domains, but not that in the non-raft domains, could induce productive infection. However, the latter possibility is unlikely, because CXCR4 in raft domains was detected in the unexposed cell–cell contact sites in TE671 cells, and NP2 and TE671 cells are as susceptible to the CD4-independent virus infection as 293T cells, in which CXCR4 is mainly localized to the raft domains. However, the CD4-independent infection in 293T cells was suppressed by MβCD as significantly as that in NP2 and TE671 cells. Because CXCR4 is originally localized to raft domains in 293T cells, the MβCD treatment could inhibit clustering the raft domains containing CXCR4 molecules in 293T cells. Taken together, clustering of the CXCR4 in raft domains should be important for the HIV-1 infection.

Why does the MβCD have no effect on the CD4-dependent infection in CD4-expressing cells? The lack of prominent inhibitory effect in our CD4-dependent infection system is compatible with previous study (Viard et al., 2002). The study showed that MβCD had no significant inhibitory effects on CD4-dependent infection when the cells expressed exogenously abundant amounts of CD4. One plausible explanation is that CD4 support the CXCR4 clustering in raft domains after the HIV-1 binding. The interaction of gp120 to CD4 could induce signals to recruit CXCR4 to cluster at the virus-binding site by regulating cytoskeleton dynamics (Iyengar et al., 1998; Viard et al., 2002; Kubo et al., 2008). It has been reported that the MβCD treatment slightly decreased cholesterol levels of the target cells (Lu

lane	effector cell	target cell
tat	tat	LTR-LacZ
untreated	tat-Env	LTR-LacZ
MβCD	tat-Env	LTR-LacZ MβCD
MβCD+chol	tat-Env	LTR-LacZ MβCD+chol

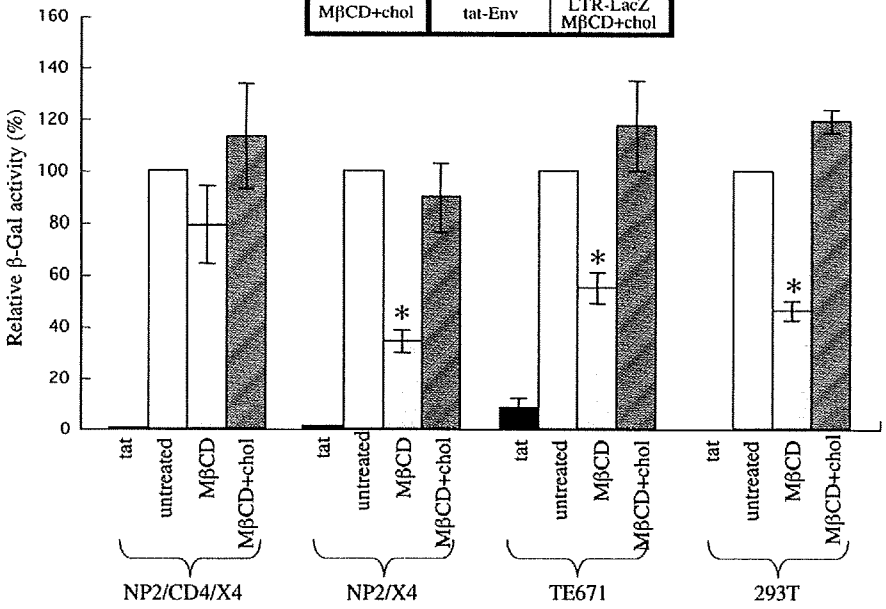

Fig. 4. Effect of MβCD on HIV-1 Env-mediated fusion. HEK293T effector cells were transfected with the tat or mNDK Env expression plasmid. The mNDK Env expression plasmid is designated as tat-Env, because it encodes the Tat protein as well as the Env protein. The target cells were transfected with the plasmids and treated by MβCD alone or both of MβCD and cholesterol as indicated in upper panel. These cells were mixed and LacZ activities of the cell lysates were measured as shown in Materials and methods. Relative values to LacZ activity of untreated cells were indicated. Asterisks indicate statistically significant differences compared to their controls.

et al., 2002), indicating that raft domains still exist in the MβCD-treated cells. Even the partial restriction of raft domains by MβCD should significantly inhibit the CD4-independent infection without the CD4 support, because certain numbers of the receptor molecules are required for the infection. Because the sCD4-induced infection was significantly inhibited by MβCD, the cytoplasmic domain-lacking sCD4 could not induce the signals. Further studies are needed to clarify this issue.

There are many evidence showing that the HIV-1 gp120-CD4-coreceptor complexes are clustered in the raft domains. However,

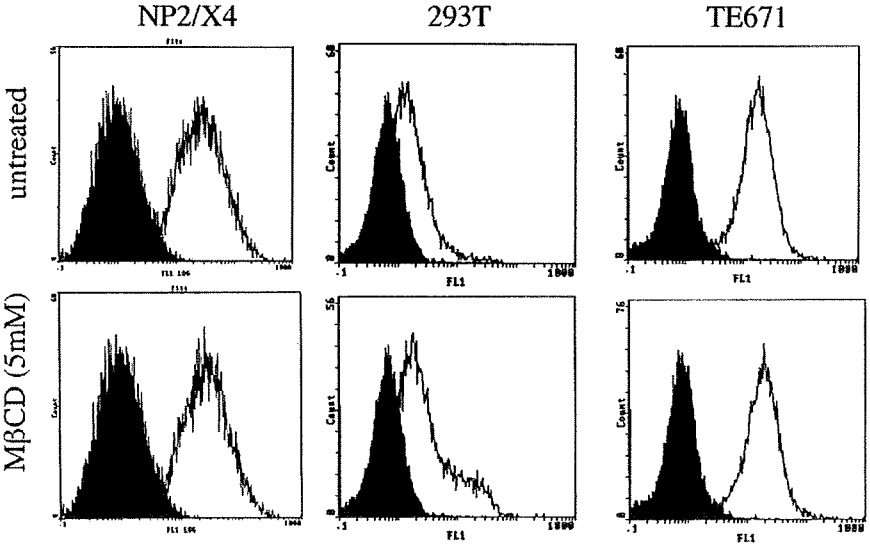

Fig. 5. Effect of MβCD on CXCR4 expression. Cell-surface expression of CXCR4 in NP2/X4, 293 T, and TE671 cells was analyzed by a flow cytometer. Upper panels indicate CXCR4 expression in untreated cells as control, and bottom panels indicate CXCR4 expression in MβCD-treated cells. Closed and open areas indicate cells that were incubated in absence and presence of the 1A80 antibody, respectively.